Marine Geology 445 (2022) 106735

Contents lists available at ScienceDirect

Marine Geology

journal homepage: www.elsevier.com/locate/margo

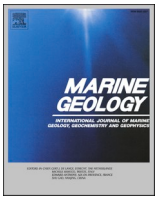

On the paleo footprint of Cape Darnley Bottom Water off MacRobertson Land Shelf, East Antarctica

Ricarda Nielsen *, Gabriele Uenzelmann-Neben

Alfred-Wegener Institute, Helmholtz Center for Polar and Marine Sciences, Germany

ARTICLE INFO

Editor: Michele Rebesco

Keywords:
Cape Darnley Botom Water
Mixed-drift formation
MacRobertson Land shelf – Prydz Bay
Seismic reflection data
Deep-sea sediments

ABSTRACT

Cape Darnley Bottom Water (CDBW) is a major contributor to Antarctic Bottom Water (AABW) formation in the MacRobertson Land continental shelf area, East Antarctica. As the production of CDBW is dependent on intense sea ice formation in the Cape Darnley Polynya Region, it is sensitive to climatic changes, such as global warming. Studying paleo-conditions of CDBW during Antarctica's transition from coolhouse to icehouse during the middle to late Miocene allows to gain knowledge about the onset of bottom water production in the Cosmonaut/Prydz Bay region as well as changes in the strength and outflow path of the CDBW.

In order to study the paleo-conditions of the CDBW, we have investigated the formation history of a 200 km long, 70 km wide sediment drift (Darnley Drift herein) at the western flank of Wild Canyon. In the early Miocene, the upper rise was dominated by turbiditic channel-levee growth and large continental sediment supply off the MacRobertson Land continental shelf. Therefore, no indications of CDBW formation were observed. During the middle Miocene, the dominant sediment transport regime transformed from turbiditic to contouritic mode, mirroring Antarctica's climatic transition into an icehouse world. This climatic transformation caused the initiation of CDBW, which is inferred from the onset of Darnley Drift formation as a levee-drift and its growth to a maximum areal extent of 60,000 km^2, four times the size of today. Since the late Miocene/early Pliocene the sedimentation rate has been strongly reduced and bottom current controlled deposition dominated. The growth of mixed levee-drifts along the continental slope-rise transition parallel to Darnley Drift suggests an intensification of paleo CDBW generation and outflow to be comparable to observations of recent CDBW, in addition to an intensification of the Antarctic Slope Front and Circumpolar Deep Water.

1. Introduction

Recent changes of Cape Darnley Bottom Water (CDBW), such as freshening (Aoki et al., 2020) and seasonal evolution of velocity, temperature and salinity (Mizuta et al., 2021; Ohshima et al., 2013), have been observed in CTD and mooring data and image its sensitivity to present-day climatic changes. CDBW is formed in the polynya north of Cape Darnley, separating the MacRobertson Land shelf area and Prydz Bay (Fig. 1), where dense shelf water formation is caused by brine rejection and outflow along Wild Canyon and Daly Canyon has been observed (Ohshima et al., 2013; Williams et al., 2016; Wong and Riser, 2013). Numerical simulations (Nakayama et al., 2014) and mooring stations (Ohshima et al., 2013) have shown that CDBW covers a depth of ~2000 to 2600 m at the continental slope-rise transition and spreads northwestwards with its deepest part reaching approximately ~4900 m (Aoki et al., 2020). It is estimated to contribute around 6–13% to the total circumpolar Antarctic Bottom Water (AABW) (Ohshima et al., 2013).

AABW is a dense cold water mass generated by mixing Circumpolar Deep Water (CDW) and Dense Shelf Water (DSW), and plays a key role within Meridional Overturning Circulation (MOC) processes (Orsi et al., 1999), which is a density and temperature driven global circulation strongly sensitive to climatic changes (Rahmstorf, 2006). Studying paleo conditions and interactions of AABW formation processes and changes during paleo warm-and cold phases is therefore essential to understand recent and future changes of the global thermohaline circulation under higher than today CO_2 concentration.

Along the continental shelf of Antarctica three regions of strong DSW formation and mixing into AABW are well known: the Weddell Sea, the Ross Sea, and the Adélie and George V Land coast (Gill, 1973; Jacobs et al., 1970; Orsi et al., 1999; Rintoul, 1998; Williams et al., 2008). In contrast to the DSW formation in regions with a large continental shelf

* Corresponding author.
E-mail address: ricarda.nielsen@awi.de (R. Nielsen).

https://doi.org/10.1016/j.margeo.2022.106735
Received 1 October 2021; Received in revised form 13 January 2022; Accepted 20 January 2022
Available online 25 January 2022

such as the Weddell Sea (Gill, 1973) and Ross Sea (Jacobs et al., 1970), CDBW outflow is representative for DSW formation on a narrow continental shelf similar to the Adélie and George V Land coast (Williams et al., 2010; Williams et al., 2008).

This study aims to investigate the paleo-evolution of the CDBW, its onset and changes in strength and occurrence during warm and cold periods since the Oligocene-Miocene transition. This knowledge will help to understand long-term changes of CDBW due to undergoing climate change and to provide boundary conditions for future CDBW and AABW oceanographic models. Investigating CDBW outflow through the transition from coolhouse to icehouse at 13.9 Ma (Westerhold et al., 2020) further allows to draw conclusions about DSW production under different climate conditions and thus sea-ice cover and glaciation of the East Antarctica along MacRobertson Land shelf.

In order to study the paleo-conditions of CDBW, we investigate the formation history of a previously unnamed drift body at the western flank of Wild Canyon (Fig. 1), the Darnley Drift (DD). The identification and interpretation of characteristic turbiditic channel-levee grow patterns and bottom current induced drift formation stages, allows to draw conclusions about the prevailing current scenario (e.g., Faugères et al., 1999; Faugères and Stow, 2008; Stow et al., 2002). We utilize a combination of around 13.350 km of multi-channel seismic reflection data available from the Seismic Data Library System (SDLS) (Wardell et al., 2007) and geological data provided at ODP Leg 188 Site 1165 (Shipboard Scientific Party, 2001b) to obtain a spatial image of the drift and possible chronological modifications.

2. Geological setting

The continental shelf along MacRobertson Land (60° – 68° E) (Fig. 1) extends about 400 km to the west of Prydz Bay, separated by the Fram Bank (depth ~ 200 m) north of Cape Darnley. The approximately 90 km wide shelf (Harris and O'Brien, 1996) has a complex morphology consisting of shallow banks (depth < 200 m) separated by apparently isolated basins that were formed by glacial erosion (Harris and O'Brien, 1996; Stagg, 1985) and may reflect interaction of the glaciers with westward flowing winds and currents (O'Brien et al., 2014). The outer shelf and upper slope were further described as iceberg-gouged and current reworked areas (Harris and O'Brien, 1996, 1998). The shelf break is sharp, with very steep slopes (7°-13°) below 600 m and extensive canyon development (e.g. Wild canyon, Daly Canyon) along the slope-rise boundary (Stagg, 1985).

Bathymetric maps show the occurrence of major mounds off Prydz Bay and MacRobertson Land shelf areas, named Wilkins Drift and Wild Drift (summarized as WD) (Fig. 1b), and Darnley Drift to the West. The deposition history of WD has been strongly affected by the interplay of glacial and interglacial sediment input along the Prydz Channel via Prydz Bay shelf bottom currents (Kuvaas et al., 2004; Kuvaas and Leitchenkov, 1992). Studies of geometry and character of the seismic reflection pattern suggest an initiation of turbidite sedimentation in late Eocene/early Oligocene when the Amery Ice shelf reached the shelf edge for the first time and intensification of current controlled deposition since the Oligocene/Miocene (Kuvaas and Leitchenkov, 1992). Major WD sedimentation during the early- to mid-Pliocene is connected to the formation of the Prydz Channel Fan by a complex of prograding sequences (O'Brien et al., 2004; Stagg, 1985; Whitehead et al., 2006).

Darnley Drift, located west of Wild drift separated by Wild Canyon (Williams et al., 2016), is shielded from direct influences and sediment input of the Prydz Bay Gyre (PG) and Dense Shelf Water (DSW) via the shallow (~200 m) Fram Bank (Fig. 1). Thus, its formation history differs from WD's because it presumably depends on the outflow of CDBW prolongating from the Cape Darnley Polynya along Wild Canyon (Ohshima et al., 2013; Williams et al., 2016).

3. Oceanographic setting

The oceanographic setting in Prydz Bay, the MacRobertson Land Shelf area and the Cooperation Sea is characterized by various currents, front systems, surface, intermediate, deep and bottom waters, schematically summarized in Fig. 1. Driven by the prevailing westerlies, the Antarctic Circumpolar Current (ACC) flows eastwards north of 63°S (Smith et al., 1984). Blocked by the topography of the Kerguelen Plateau

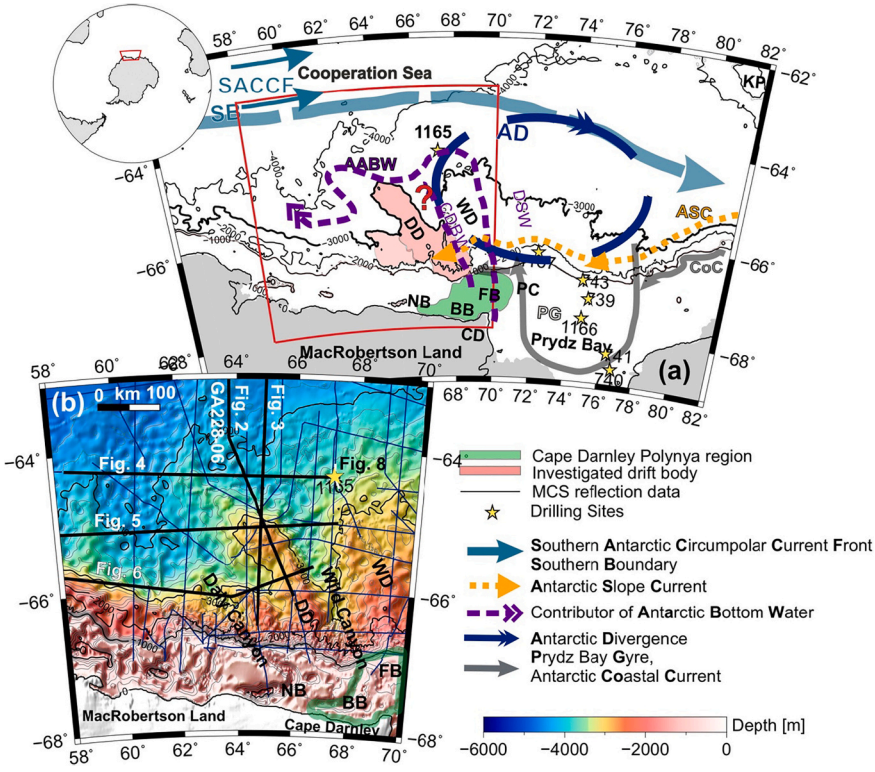

Fig. 1. (a) Overview map of Prydz Bay continental shelf (PB), MacRobertson Land shelf and Cooperation Sea (CS) area, East Antarctica. Prevailing currents: Antarctic Slope Current (ASC), Antarctic Coastal Current (CoC), Prydz Bay Gyre (PB). Front systems: Southern Antarctic Circumpolar Current Front (SACCF) with Southern Boundary (SB), Antarctic Divergence Zone (AD). Water masses: Antarctic Bottom Water (AABW), Dense Shelf Water (DSW), Cape Darnley Bottom Water (CDBW). Drift Bodies: Investigation area (red box) of Darnley drift (DD), Wilkins drift and Wild drift (summarized as WD) separated by Wild Canyon north of Cape Darnley (CD) Polynya region (green highlighted area) and Prydz Bay shelf. Other abbreviations: Fram Bank (FB), Prydz Channel (PC). Kerguelen Plateau (KP), Burton Basin (BB), Nielsen Basin (NB). ODP Leg 188 Site 1165 is marked with a yellow star. Panel (b) shows bathymetry in the investigated area and overview of used multi-channel seismic (MCS) reflection data (thin solid blue lines) and displayed seismic data (black thick lines). (For interpretation of the references to colour in this figure legend, the reader is referred to the web version of this article.)

(KP), the Southern Antarctic Circumpolar Current Front is shifted south to pass through the Princess Elizabeth Trough. It transports Antarctic Surface Water, CDW and AABW originating from the Weddell-Enderby Basin (Heywood et al., 1999; Orsi et al., 1995).

Driven by the continental Easterlies, the Antarctic Slope Front (Jacobs, 1991) can be observed along and just below the shelf break. This topographically controlled front is associated with a westward flowing double-banded frontal jet. It separates Eastern Shelf Water from Antarctic Surface Water in the surface layers (Middleton and Humphries, 1989) and Circumpolar Deep Water and AABW in the deeper layers (Heywood et al., 1999).

On the shelf, a narrow westward flowing Antarctic Coastal Current (CoC) enters Prydz Bay, forms the Prydz Gyre (Smith et al., 1984), and splits, one part leaving Prydz Bay towards the west in a strong current with velocities ~1 m/s along MacRobertson Land Shelf and another part flowing offshore towards the North, mixing with the ASC and modified CDW and recirculating clockwise (Borchers et al., 2011; Vaz and Lennon, 1996).

The transition zone between the Southern Boundary (SB) of the ACC (Orsi et al., 1995) and the westward flow near the Antarctic continental shelf is called the Antarctic Divergence (AD) (Vaz and Lennon, 1996), which develops a series of large gyres with a band of westward-flowing waters (Smith et al., 1984). They cause upwelling of warmer saline CDW. Wakatsuchi et al. (1994) identified a large gyre centered at ~68°E with dimensions of ~500 km in the zonal and 200 km in the meridional direction.

It has long been controversially discussed, whether bottom water is produced in Prydz Bay and to what extent it contributes to AABW (Vaz and Lennon, 1996 and references therein). Today, DSW is produced below the Amery Ice Shelf and prolongates along the Prydz Channel. However, Fram Bank in the West acts like a barrier, and thus only limited water mass exchange and outflow takes place along Prydz Channel as AABW (Bindoff et al., 2000; Smith et al., 1984; Vaz and Lennon, 1996; Williams et al., 2016).

Modern DSW production was confirmed in the Cape Darnley polynya region adjacent to Prydz Bay and northward outflow as CDBW along the Wild Canyon and Daly Canyon (Nakayama et al., 2014; Ohshima et al., 2013; Williams et al., 2016). CDBW spreads northwestwards in the Cooperation Sea with its deepest part reaching approximately ~4900 m (Aoki et al., 2020). Ohshima et al. (2013) estimated that approximately 0.3–0.7 $\times$ 10^6 m^3 s^{-1} of DSW produced in the Cape Darnley polynya is transformed into AABW, which accounts for 6–13% of the total AABW production.

4. Data and methods

4.1. Multi-channel seismic reflection data

To investigate the sedimentary structure of Darnley Drift and the surrounding area, we interpreted around 13.350 km of multi-channel seismic reflection (MCS) data (Table 1, Fig. 1, Figs. 2-6). The MCS data were provided by the Antarctic Seismic Data Library System (SDLS) (Wardell et al., 2007).

The provided data (Table 1) are stacked, deconvolved, band-pass filtered (5–120 Hz, peak at 30 Hz or 70 Hz) and applied with automatic gain control (AGC) using time variant windows that differ in length for different surveys. Detailed information on the individual surveys can be found in previous publications or in the SDLS database (Joshima et al., 2001; Kuvaas and Leitchenkov, 1992; Mizukoshi et al., 1986; Stagg, 1985; Wardell et al., 2007). The data quality varies due to differences in acquisition parameters as well as processing steps and the usage of filter and AGC length. However, the amplitude spectra and the two-way-traveltime (TWT) of key horizons like the seafloor, the basement and seismic sequences are consistent at cross-sections. Thus, we were able to trace prominent horizons from one survey to another at cross-points and combine the surveys to obtain a pseudo 2.5D image of the sedimentary structure offshore MacRobertson Land.

4.2. Lithology obtained from ODP drill sites

Wild Drift, located east of Darnley Drift (Fig. 1), has been sampled at ODP Leg 188 Site 1165 (999 m maximum penetration) (Table 2 and Fig. 8) and provides a mostly continuous record of Oligocene to Quaternary sediments recording the development of the EAIS and its interplay with the ocean bottom current systems (Hannah, 2006; Passchier, 2011; Shipboard Scientific Party, 2001b). Overall, three lithostratigraphic units I (0–63.8 mbsf), II (63.8–307.8 mbsf) and III (307.8–999 mbsf) have been identified (Fig. 8 and Table 2), with each unit being characterized by cyclic variations between biogenic-bearing and terrigenous-dominated intervals (Shipboard Scientific Party, 2001b).

Unit I (0–6 Ma) primarily contains structureless laminated clay, claystone and diatoms. The occurrence of dropstones and dispersed sand grains indicates ice rafting during its deposition (Shipboard Scientific Party, 2001b). Sedimentation rates are 10–15 m/My (Florindo et al., 2003).

Unit II (6–14.3 Ma) contains structureless clay, claystone and diatoms. It has been subdivided into three Subunits IIA (63.8–160 mbsf), IIB (160–252.4 mbsf), and IIC (252.4–307.8 mbsf), partially based on a greater amount of Ice-Rafted-Debris in Subunits IIA and IIC (Shipboard Scientific Party, 2001b). Sedimentation rates increase downhole from

Table 1
Multichannel seismic reflection (MSC) data used in this study to investigate the Darnley Drift and surrounding area in the Prydz Bay region. Data were provided by the Antarctic Seismic Data Library System database (https://sdls.ogs.trieste.it/) (Wardell et al., 2007).

	Country	Year	Reference, cruise leader	Source Type Airgun	Sample rate [ms]	Shot/CDP Interval [m]	fold	km	Number of profiles
BMR33	BMR Australia	1981	Stagg	460 cu. in.	4	25, 50	3, 6	1100	3
GA228	Geoscience Australia	2002	Stagg	60 l	4	12.5	36	950	4
GA229	Geoscience Australia	2002	Stagg	60 l	4		36	1450	5
RAE40	PMGRE Russia	1995	Gandyukhin	2440 cu.in.	4	25, 50	24	3000	1
RAE47	PMGRE Russia	2002	Leitchenkov	2440 cu.in.	4	50	18	4208	12
TH84	JNOC Japan	1984	Ohuda, Tanakashi	800 cu.in.	4	50	6	450	4
TH99	JNOC Japan	2000	Ohuda, Tanakashi	4000 cu.in.	4	50	30	2195	10

Table 2
Information of Site 1165 are taken from (Shipboard Scientific Party, 2001a, 2001b), ages have been defined by [1]Florindo et al. (2003) and [2]Hannah (2006). Previously defined seismic stratigraphy: [3]Stagg (1985), [4]Mizukoshi et al. (1986), [5]Kuvaas and Leitchenkov (1992), [6]Handwerger et al. (2004), [7]Shipboard Scientific Party (2001b), [8]Cooper and O'Brien et al. (2004), [9]Leitchenkov et al. (2007). In this study, we defined reflectors CS4a-CS9 and the corresponding seismic units. The colours in the table link to the horizons displayed in the seismic profiles.

Leg 188 Site 1165					Seismic Stratigraphy			Time	Interval velocity
Unit (m)	Subunit	Depth (mbsf)	Age[1]	Sedimentation rate[1] (m/My)	Seismic sequences[3]	Seismic Unit this study	Horizon this study/ previous studies	ms TWT	m/s
		0					CS9	4809	
Unit I 0 – 63.8				10 - 15		CS9-CS8			
		63.8	~6 Ma				CS8/A[4]/PP-12[5,7]	4857.2	1500
	Subunit IIA			20		CS8-CS7b			
		114	8 Ma[2]		PD1		CS7b	4917.5	
Unit II 63.8 – 307.8		160.1				CS7b-CS7	CS7a	4972.0	
	Subunit IIB			37					1600[7]
		252.4	~11.7 Ma				CS7	5082.2	
	Subunit IIC					CS7-CS6			1800
		307.8	~14.3 Ma				CS6/B[4]	5147.4/~5250[6]	
				70					
		492.2	~17 Ma				CS5c	5357.3	
		600		120[7]	PD2	CS6-CS5	CS5b	5475.1/ 5560-5660[6]	2000
Unit III 307.8 – 999.1		692	~19 Ma				CS5a	5569.5	
		907	~21.8 Ma		PD2/PD3		CS5/P3[8]	5782.1	
					PD3				2660-2840[7]
		Not drilled	~24 Ma[9]			CS5-CS4	CS4a/P2[5]/ CS5[9]	6100	
		Not drilled	Eo/Oli		PD3/PD4?		CS4/P1[7]/CS4[9]		

20 m/My in subunit IIA to 37 m/My in subunits IIB and IIC (Florindo et al., 2003). A notable change in the palynological composition has been found between 99.1 and 310 mbsf, where any in situ palynomorphs are almost absent and reworked marine and terrestrial palynomorphs dominate (Hannah, 2006). Hannah (2006) concluded that this interval represented a significant climatic shift, including a dramatical ice shelf expansion.

The transition between Unit II and Unit III (308 mbsf, age ~ 14.3 Ma) is characterized by significant up-hole changes: an increase in the total clay content, an increase of the amount of sand-sized and dropstone Ice-Rafted-Debris and an eightfold decrease in average sedimentation rates (Florindo et al., 2003; Shipboard Scientific Party, 2001b). This transition has been explained to represent a mid-Miocene (Shipboard Scientific Party, 2001b) sharp climatic reversal resulting in the formation of a permanent Antarctic Ice Sheet.

Unit III contains planar laminated clay, claystone and diatoms, as well as partly alternating facies of sand grains and rare granule to pebble sized dropstones. Multiple cycles of glacial activity and expansion of ice at 990–830 mbsf (22.2–20.8 Ma), 830–690 mbsf (20.8–19 Ma), and 690–310 mbsf (19–15 Ma) (Cooper and O'Brien, 2004; Hannah, 2006; Shipboard Scientific Party, 2001b) resulted in sedimentation rates ranging between 70 m/My in the upper Unit III to 120 m/My in the lower unit (Shipboard Scientific Party, 2001b).

4.3. Extension of existent seismostratigraphic model

A first seismostratigraphic model for the Prydz Bay shelf (PS1-PS6) and abyssal plain area (PD1-PD5) was defined by Stagg (1985) and has later been modified (Cooper et al., 1991; Erohina et al., 2004; Joshima et al., 2001; Kuvaas and Leitchenkov, 1992; Leitchenkov et al., 2007; Leitchenkov et al., 1994; Mizukoshi et al., 1986; Whitehead et al., 2006) based on seismic reflection patterns and lithostratigraphic correlation (overview in Table 2). It distinguishes six seismic units in the shelf region (PS) and five seismic units in the abyssal plain (PD), ranging in age from the Cambrian or older (PS6) to Pliocene and younger (PD1) (Stagg, 1985).

Spatial correlation of the previously published seismic stratigraphy at seismic line SAE3306 (Shipboard Scientific Party, 2001b) and single channel seismic data (Handwerger et al., 2004) to the seismic dataset used in this study was impossible, as those datasets were not available in the SDLS database (Wardell et al., 2007). We therefore calculated a synthetic seismogram and identified additional key horizons, which were correlated to lines GA228–07, RAE47-06A and TH99–26 crossing Site 1165 (Fig. 8, Table 2). To calculate the impedance logs, we used bulk density and a composite P-wave velocity log obtained from cores and borehole logs of ODP Site 1165 provided and described by Handwerger et al. (2004). The log files consist of datapoints every 1 m in the upper 0–204 m depth and ~ 0.2 m intervals below 204 m to the bottom of the drill site. The data were convolved with a Ricker-wavelet that had a signal frequency band between 10 and 100 Hz obtained from spectral analysis of the seismic data crossing Site 1165 (lines GA228–07, RAE47-06A and TH99–26).

The defined nomenclature follows Leitchenkov et al. (2007) naming the reflectors from oldest to youngest with Cooperation Sea (CS) as prefix (Fig. 8). Our seismostratigraphic model consists of seven key horizons CS4a to CS9 (Fig. 8, Table 2). A detailed correlation of previously published horizons to the newly defined horizons is given in Table 2. The interpreted seismic units are referred to by the lower-upper bounding reflectors, CS5-CS6, CS6-CS7 and CS7-CS9 (Table 2), respectively.

4.4. Depth and isopach maps

We provide depth slices in ms TWT (Fig. 7a-d) of key horizons CS5 to CS9 and thicknesses of their associated seismic units CS5-CS6, CS6-CS7 and CS7-CS9, respectively, displayed as isopach maps in ms TWT

(Fig. 7e-g) to obtain a view of the growth stages, specifically the spatial extent and changes of the depositional regime of Darnley Drift. We used the root-mean-square value of depth and thickness, respectively, to evaluate lateral and vertical changes for the individual seismic sequences based on depositional pattern and geometry of the features (marked as thick black lines in Fig. 7). We maintained our grid using the near-neighbor function in GMT (Wessel and Luis, 2017) with nodes every 2 km and bin size with radius of 25 km. Due to the resolution limits, we concentrate on observed structures larger than 50 km. We interpret orientations of depocenters following Uenzelmann-Neben (2006), with mainly along-slope transport resulting in depocenters parallel to the continental slope or down-slope transport for depocenters perpendicular to the slope.

4.5. Classification of seismic features

Based on published literature, the observed seismic features are classified into turbiditic channel-levee complexes or bottom current induced drifts, in order to evaluate the predominant current and formation process.

4.5.1. Channel-levee complexes

Submarine canyon-channel systems represent one type of a sediment-transfer zone between terrestrial source areas and deep-sea depositional sinks (Covault, 2011). Near the continental shelf and uppermost slope, they are generally V-shaped and continue across the lower slope and rise as U-shaped channels with overbank deposits forming levees. In the southern hemisphere, the levees are typically asymmetric with a larger levee forming along the left side downstream of the channel due to Coriolis force. Submarine lobes are formed at the channel-mouth, where turbidity currents exit channel confinement and loose load-carrying capacity (Covault, 2011; Deptuck and Sylvester, 2018). Turbidites are characterized by distinct beds with sharp bases and sharp to gradational tops that reflects a single source formation geometry. They show a variation of well-defined thin-to-thick bedded successions, which often are lenticular and discontinuous in thin beds and spaced to indistinct in thick beds (Stow and Smillie, 2020, and references therein).

4.5.2. Contouritic drift deposits

Sediment drifts are large-scale morphological expressions, formed by the action of long-lasting contour (bottom) currents (Esentia et al., 2018 and references therein; Faugères and Stow, 2008; Stow et al., 2002). Based on their overall morphology and formation setting, sediment drifts can be grouped into different classes (Stow et al., 2002): contourite sheet drift, elongated mounded drifts, channel-related drifts and modified drift-turbidite systems/mixed-drift systems. The growth and overall geometry of a drift body is principally controlled by four interrelated factors: the bathymetric framework, the velocity and variability of currents, the available amount and type of sediments and the duration of ongoing bottom current processes (Faugères et al., 1999; Faugères and Stow, 2008). Within this work we focus on (i) channel-related drifts and (ii) modified drift-turbidite systems/mixed-drift systems:

(i) Channel-related drifts are related to deep channels or gateways, where the velocity of the bottom circulation is markedly increased. This results in erosion and non-deposition within the channel. Localized patch drifts can occur within the channel, their shapes being either mounded or sheeted. At the channel exit contourite fans develop, composed of an aggradation of flat irregular lenticular depositional units.

(ii) Modified drift–turbidite/mixed drift systems are the result of interacting down-slope and along-slope processes) (Faugères et al., 1999; Stow et al., 2002). Depending on the alternation and period of dominant processes, the drift exhibits an asymmetric channel levee structure with larger levees and extended tail in the direction of the dominant bottom current flow (Faugères et al., 1999; Stow et al., 2002). Contour currents induce a downstream lateral shift of the turbiditic levees depending on the strength of the current (**Error! Reference source not found.**d) and can even result in areas of non-deposition or erosion of the turbiditic lobe deposits (Faugères et al., 1999).

5. Results

5.1. Revised seismic stratigraphy

Our seismostratigraphic model consists of seven key horizons CS4a to CS9 ranging from the Oligocene/Miocene boundary (Kuvaas and Leitchenkov, 1992; Leitchenkov et al., 2007) to present day (Fig. 8, Table 2). Horizon CS4a corresponds to horizons P2 and CS5 defined by (Kuvaas and Leitchenkov, 1992) and (Leitchenkov et al., 2007), respectively, and has an age of around 24 Ma.

Horizon CS5 forms the base of seismic unit CS5-CS6 and is located at 907 mbsf/5782 ms TWT at ODP Leg 188 Site 1165. It corresponds to horizon P3 of Cooper and O'Brien (2004) (Table 1). Horizon CS5 represents the Oligocene/Miocene boundary and can be identified by a downhole decrease in total clay and an increase in silt content (Handwerger et al., 2004; Shipboard Scientific Party, 2001b). Seismic unit CS5-CS6 corresponds to lithological Unit III at ODP Site 1165, which is formed by a large sediment supply originating from multiple ice-advance events on the shelf (Cooper et al., 2008; Hannah, 2006; Shipboard Scientific Party, 2001b).

Horizon CS6 (307 mbsf/ 5147 ms TWT at Site 1165, Fig. 8, Table 2) is an unconformity that marks the base of seismic unit CS6-CS7 and represents the transition from lithological Unit III to Unit II at ODP Site 1165. Reflector CS7 (252 mbsf/5082 ms TWT at Site 1165, Fig. 8) is an erosional unconformity, corresponding to the boundary of subunits IIB/IIC, above which the characteristic of the sedimentary sequence CS7-CS9 changes to be of an overall uniform thickness and well layered. At ODP Site 1165, sedimentation rates further decrease to 10 m/My above this boundary (Cooper et al., 2008).

5.2. Seismic unit CS5-CS6

In the seismic profiles perpendicular to the continental shelf (Figs. 2-3), unit CS5-CS6 consists of parallel to subparallel continuous reflector packages of varying thickness that alternate with thick transparent convex-mounded subsequences, especially towards the continental slope. We observe an overall thinning of the sequence towards the abyssal plain, except for an elongated mounded structure (CDP 5500–7500 in Fig. 3) with a diameter of ~60 km. On the middle continental rise, perpendicular to Wild Canyon, a channel can be identified showing erosion and cut-and-fill features (grey area centered at CDP 18000 in Fig. 2 and CDP 4500 in Fig. 3).

In the seismic profiles parallel to the continental shelf (Fig. 4-Fig. 6), inner-sequence reflectors are subparallel and mostly continuous. We observe an alternation of transparent subsequences and well-layered reflectors. At the continental slope-rise transition, a channel-levee system is developed at horizon CS4a (CDP 7000 in Fig. 4). Above horizon CS4a, a cut-and-fill feature can be observed at Wild Canyon flanked by asymmetric levees that are partly eroded (CDP 4000–7500 in Fig. 4). The larger western levee has a steep flank towards the channel axis and a gentler tail towards the west.

In the depth slice of horizon CS5 (Fig. 7a) a series of seaward convex mounded sediment lobes off MacRobertson Land shelf are visible, which thin towards the abyssal plain. The depth slice has a rms depth of 6640 ms TWT (thick black line in Fig. 7a). Seismic unit CS5-CS6 (Fig. 7e) has a thickness of ~200 ms TWT along Wild Canyon and more than 1000 ms TWT on the adjacent levees. Based on a mean thickness of 432 ms TWT (thick black line in Fig. 7e) and average velocity of 2000 m/s (Table 2), we have calculated a sedimentation rate of 86 m/My for seismic unit

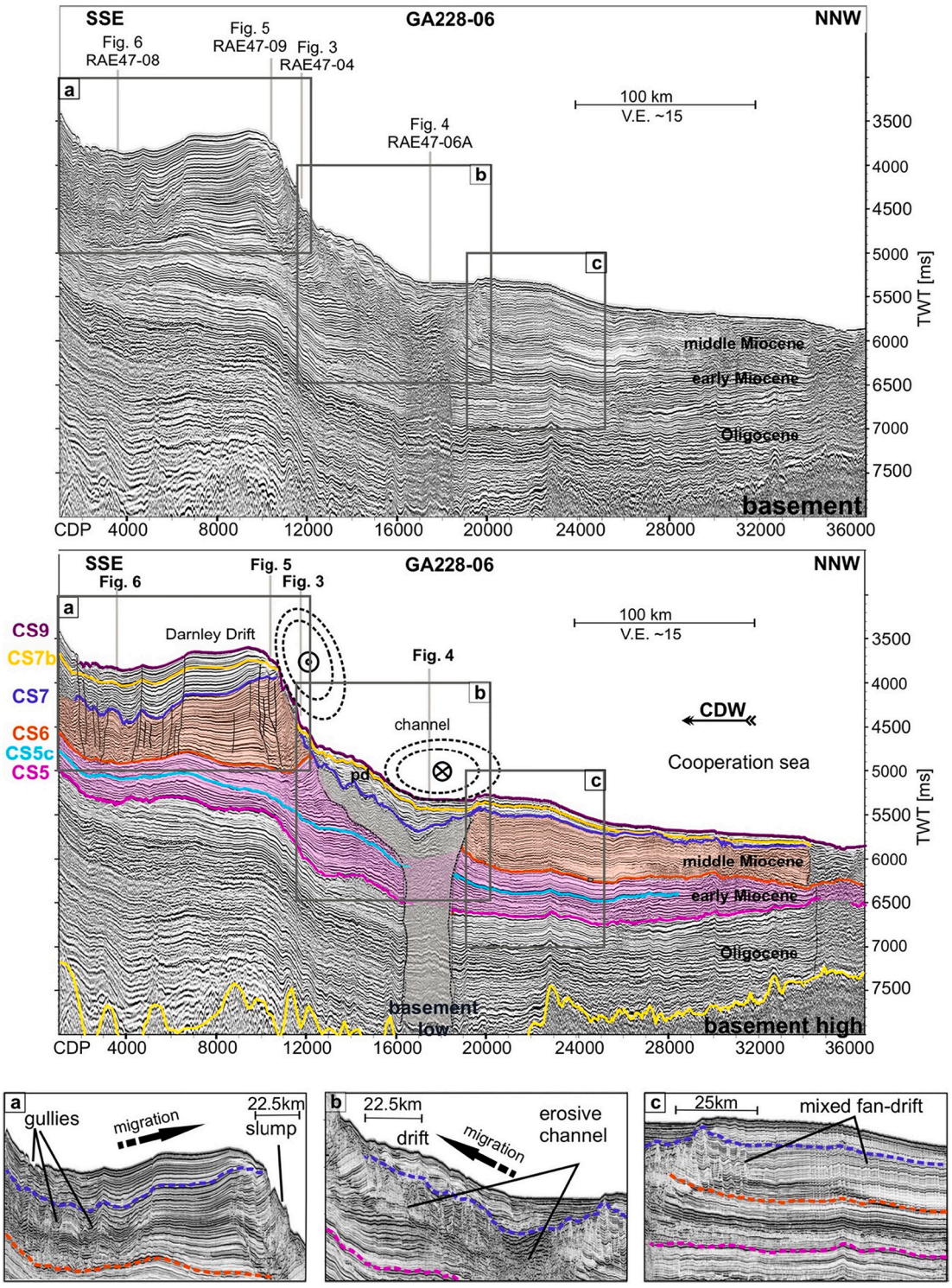

Fig. 2. Seismic section crossing Darnley drift and surrounding areas. The profile location of GA228–06 can be found in Fig. 1b. pd. - patch drift, black arrows show crest migration of the drift. Currents marked with cross flows into the plain, with dotted circle comes out of the plain. Grey-colored vertical zone marks channel sediments.

CS5-CS6. The overall sediment thickness thins towards the abyssal plain. At the channel mouth around 64.5°-65°S a deflection of the western levee to the west can be observed. North of the channel mouth, between 63°-64°S, the lobe is elongated towards the north and the sedimentary depocenter is shifted towards the western flank of the lobe.

5.3. Seismic unit CS6-CS7

Seismic unit CS6-CS7 (Figs. 2-6) consists of alternating transparent and well-layered parallel reflection. The thickness of the seismic unit strongly varies areal dependent. In the seismic profiles (Figs. 2-6), horizon CS6 marks an unconformity above which stacks of lenticular seismic sequences form a convex geometry with a thickness up to 1000 ms TWT, which can also be observed in the isopach map (Fig. 7f). The

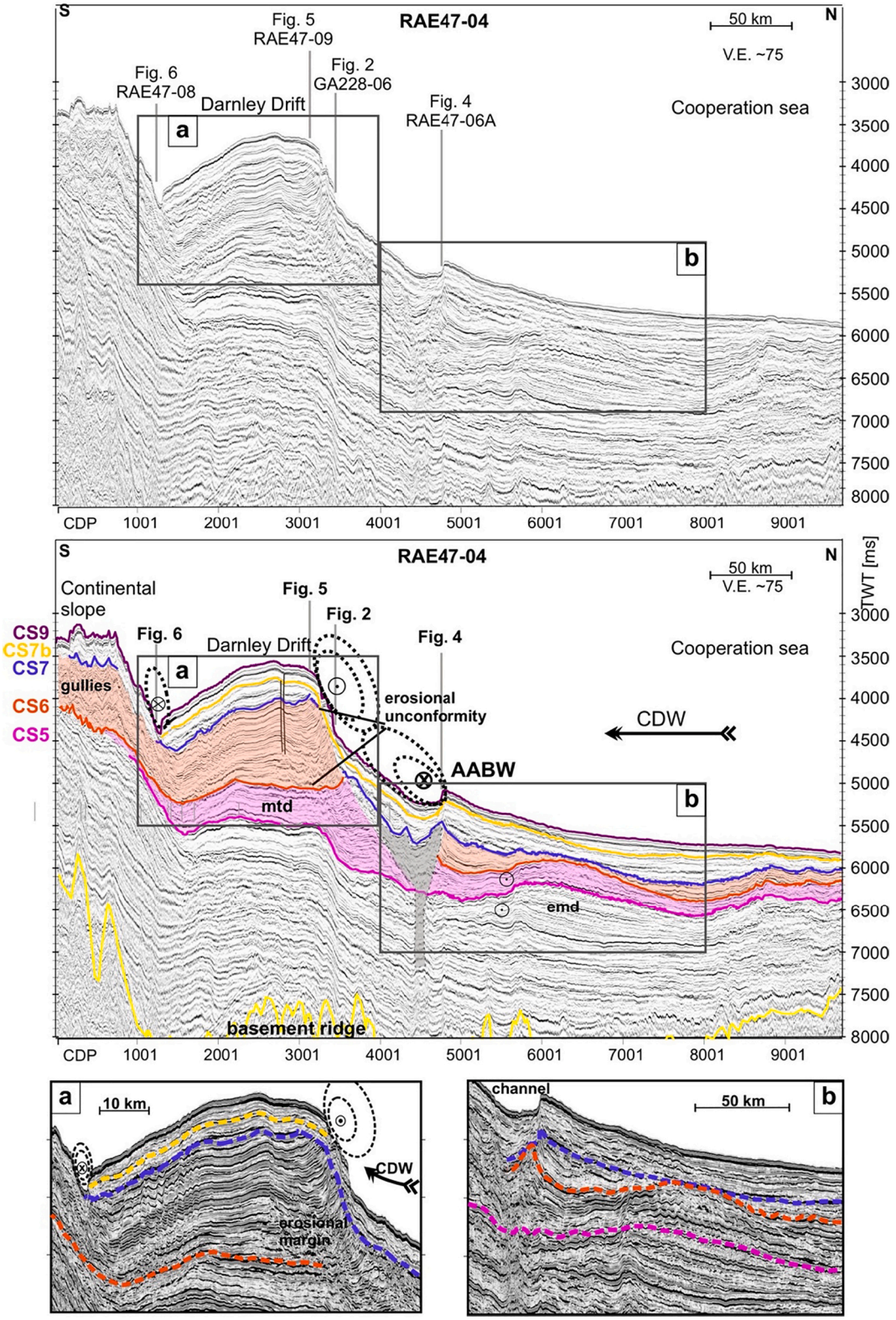

Fig. 3. Seismic section crossing Darnley drift and surrounding areas. The profile location of RAE47–04 can be found in Fig. 1b. Abbreviations: pd. - patch drift, mtd - mass transport deposit, emd - elongated mounded drift, Currents marked with cross flows into the plain, with dotted circle out of the plain. Grey-colored vertical zone marks channel sediments.

crest shows a migration towards the abys (Fig. 2 CDP 4000–12,000, Fig. 3 CDP 1500–3500). The sedimentary body is terminated by erosion and an ~75 km wide channel similar to Wild Canyon (cut-and-fil structure). North of the channel reflectors are well-layered, continuous and parallel with localized transparent zones (Fig. 4), which we interpret to be a mixed-fan-drift.

Gullies occur in the southeastern part of the drift in seismic unit CS6-CS7 (Fig. 2, CDP 1200–6000), whereas a 2–3 km wide channel trending

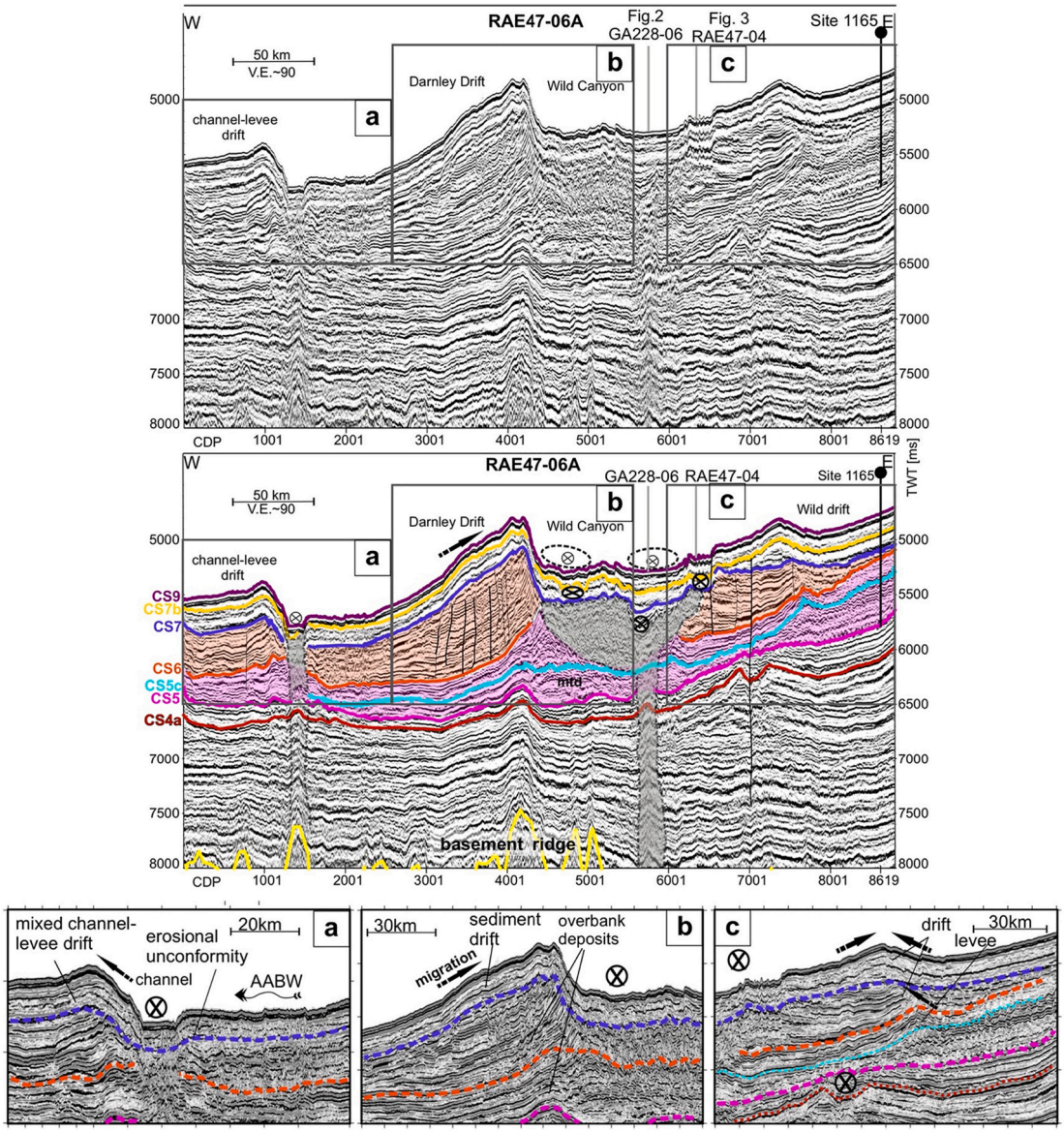

Fig. 4. Seismic section crossing Darnley drift and surrounding areas. The profile location of RAE47-06A can be found in Fig. 1b. ODP Site 1165 is marked with the symbol. Abbreviations: mtd - mass transport deposit, emd - elongated mounded drift, show migration of the drift crest. Currents marked with cross flows into the plain, with dotted circle out of the plain. Grey-colored vertical zone marks channel sediments.

parallel to the continental slope can be observed in the southwest accompanied by small scale faults (CDP 1200–2200 in Fig. 3).

In east-west direction (Fig. 4-Fig. 6) Darnley Drift still appears as a wedge-shaped levee in the lower part of seismic unit CS6-CS7. The sequences show an alternation of transparent sub-sequences and well-defined continuous reflectors that converge away from the channel axes (CDP 1000–5000 in Fig. 4). In the upper part of seismic unit CS6-CS7, the internal reflection pattern changes to be well stratified and lenticular mounded. Reflectors in the upper part of seismic unit CS6-CS7 downlap onto the lower part of seismic unit CS6-CS7 (Fig. 5 CDP 7500–8000).

At the channel mouth ~65°E/ 65°S we observe a sinuous trend change of Wild Canyon to the west, forming a meander loop that follows the contours of the previously (seismic unit CS5-CS6) built Darnley mixed fan-drift (Fig. 7f). In the seismic data, the meander is characterized as a flat-topped, terrace-like, 50–100 km wide western channel at the channel mouth at 63°E-65°E/64.5°S (CDP 4500–5500 in Fig. 4, Fig. 7f) that is characterized as an area of non-deposition and/or erosion (Figs. 2-4, Fig. 7f). Less sedimentation is also visible in the eastern part of Wild Canyon and on Wild/Wilkins Drift.

Fig. 7b displays the depth of horizon CS6, which shows a similar shape as horizon CS5 with high elevation at the continental slope and a decrease towards the abyssal plain, but located further towards the north. Horizon CS6 has a mean depth of 5560 ms TWT (black thick line). The isopach map of seismic unit CS6-CS7 shows a sedimentary areal extent to a size of 60°-66°E/63.5°-66,5°S. Based on the mean thickness of 432 ms TWT of seismic unit CS6-CS7, we have calculated an overall sedimentation rate off MacRobertson Shelf of ~150 m/My and velocities and age values provided in Table 2.

5.4. Seismic unit CS7-CS9

Seismic sequence CS7-CS9 consists of a parallel reflection pattern of uniform thickness (Fig. 2-6) and downlaps onto horizon CS7 (e.g., CDP 8000 in Fig. 5). Localized features contain mound formation on Darnley Drift (e.g., Fig. 4) in the lower continental rise and in-fill of the western channel (CDP 4000–4500 in Fig. 3). Towards the continental slope-rise transition the slope-parallel channel has migrated towards the south

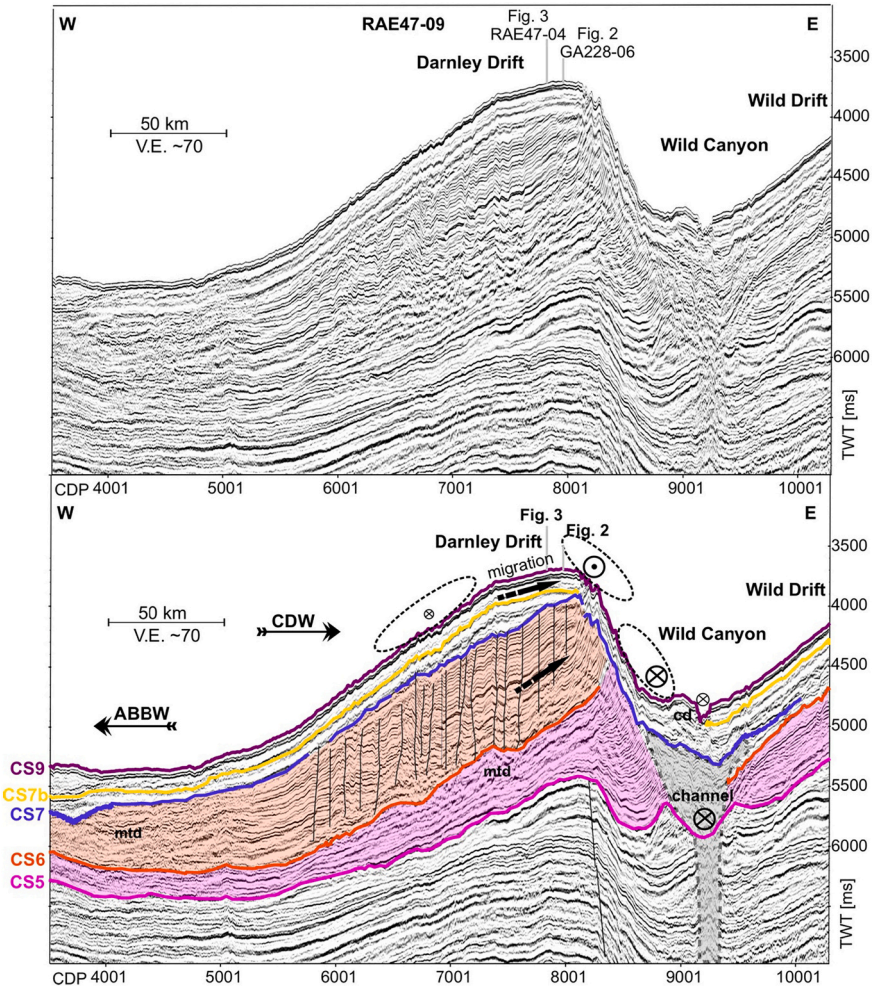

Fig. 5. Seismic section crossing Darnley drift and surrounding areas. The profile location of RAE47–09 can be found in Fig. 1b. Abbreviations: mtd - mass transport deposit, black arrows mark migration of the drift crest. Currents marked with cross flows into the plain, with dotted circle out of the plain. Grey-colored vertical zone marks channel sediments.

(CDP 1300 in Fig. 3). About 50 km north of the shelf break, slope-parallel trending high-relief, mounded sediment bodies are enlarged west of Darnley Drift (Fig. 6, Fig. 7g).

The 4431 ms TWT contour line in the depth-slice of horizon CS9 (Fig. 7c) shows Darnley Drift as a northwest elongated, detached mounded feature that terminates at ~64.5°S, at the Wild Canyons channel mouth. Separated by a channel (Fig. 2-3,Fig. 7c), a mounded circle shaped sediment accumulation ~1000 ms thick in the isopach map of seismic unit CS7-CS9 (Fig. 7g) is observed to its north at 63°E-65°E/64.5°S. The location correlates to the previously (seismic unit CS6-CS7) formed meander loop. Its symmetric geometry and internal reflection pattern showing truncations on two sides are similar to drift bodies observed in the lower rise of the Cosmonaut Sea (Kuvaas et al., 2005).

On the northern margin of Wild Drift at around 64°S/66°E-70°E, we observe a ~ 200 km long east-west elongated sediment mound, with a circle shaped center and elongated side lobes in the isopach maps of seismic unit CS7-CS9 (Fig. 7g). It is bounded to its south by another sediment accumulation with a thickness between 500 and 1000 ms TWT.

5.5. *Wild Canyon – a channel-levee complex*

Wild Canyon is a north-northwest trending ~250 km long channel-canyon complex that separates Wild Drift and Darnley Drift off MacRobertson Land (Fig. 1b and Figs. 4-6).It is ~10 km in diameter at the continental slope-rise transition (Fig. 6 CDP 10–200) and broadens northwards to ~50 km at 65°S (Fig. 5 CDP 8500–9500) and ~ 100 km at 64°S (Fig. 4 CDP 4500–6500).

In the seismic sections, a buried channel-levee system can be identified above horizon CS4a (CDP 7000 in Fig. 4) as a cut-and-fill feature (Kuvaas and Leitchenkov, 1992). Wild Canyon is formed about 50 km further west in seismic unit CS5-CS6 and the lower part of seismic unit CS6-CS7 (CDP 5600 in Fig. 4). Strong erosion of 1000–1500 ms TWT in the lower part of seismic unit CS6-CS7 (CDP 4000–5500 in Fig. 4) and in the upper part of seismic unit CS5-CS6 results in a steep flank with a sharp erosional surface at the western flank of Wild Canyon. Within Wild Canyon, erosion created a ~ 50 km wide, flat-topped western channel (CDP 4500–5500 in Fig. 4). Above erosional unconformity CS7 (CDP 4500–5500 and 5500–6500 in Fig. 4), Wild Canyon splits into two channels, a broader western one and a narrow ~5 km wide eastern one (CDP 9200 in Fig. 5). At the upper continental rise, two asymmetric levees (CDP 4000 and 7500 in Fig. 4) are developed by overbank deposition, a smaller eastern one and a larger western one. The western levee is developed above a basement ridge (CDP 3000–5000 in Fig. 4 and supplementary material), Wild Canyon above a basement low. The internal seismic reflection pattern of the levee shows an alternation of thick transparent sequences and thinner sequences above, as well as a distal transformation to thin, well-defined reflector sequences (e.g., CDP 2000–12,000 in Fig. 2, CDP 5000–9000 in Fig. 5, Fig. 7f), which is

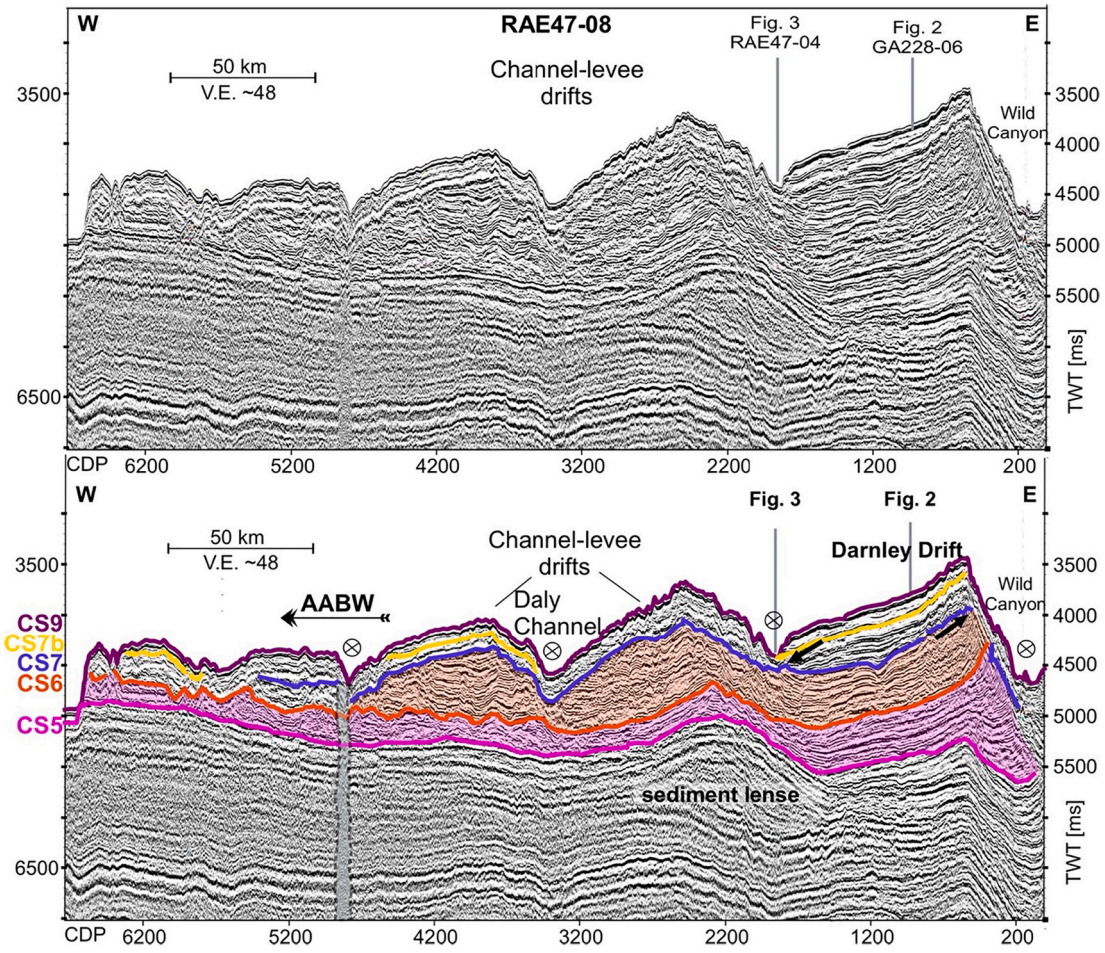

Fig. 6. Seismic section crossing Darnley drift and surrounding areas. The profile location of RAE47–08 can be found in Fig. 1b. sl- sediment lense, black arrows show onlap or downlap structures. Currents marked with cross flows into the plain, with dotted circle out of the plain. Grey-colored vertical zone marks channel sediments.

characteristic for turbiditic deposition (Deptuck and Sylvester, 2018; Stow and Smillie, 2020).

5.6. Darnley Drift body

Darnley Drift is a ~ 70 km wide and ~ 250 km long bathymetric high off the MacRobertson Land continental shelf, trending NNW from the continental slope-rise transition into the abyssal plain (Fig. 1b). It is elevated up to 2000 m above the surrounding seafloor (Fig. 1b). Along-strike MCS profiles (Fig. 2, Fig. 3) and Fig. 4 show that Darnley Drift is underlain by a basement high (supplementary material). The 3000 m bathymetric contour line (Fig. 1b) and seismic profiles (Figs. 2-6) display the drift as an elongated mounded feature with steep eastern and northern flanks and a gentler western flank. Narrow canyons of 2–3 km width at the upper continental rise and slope delimit the inner part of the drift in the south (CDP 1200 in Fig. 3) and in the west (~10 km). However, major parts of the drift are bounded by Wild Canyon in the east, separating Darnley Drift from Wild Drift, and a wide channel (western branch of Wild Canyon) of ~50 km to ~100 km width in the north, which is located above a basement low (Fig. 2, Fig. 3, Fig. 6 CDP 200, 2000). Horizon CS7 marks an unconformity, above which sediments of seismic unit CS7-CS9 fill-in the channel in a sub-parallel accumulation to form a channel drift (Fig. 3 CDP 3500–4500) that migrates south towards the Darnley Drift crest.

Horizon CS6 marks the unconformity in the seismic profiles (Fig. 2-6), above which stacks of lenticular seismic sequences form a convex geometry with a total thickness (CS6-CS7 plus CS7-CS9) of up to ~1500 ms TWT. Its tail faces the continental slope (Fig. 2 and Fig. 3) and the crest shows a migration from south to north towards the abyssal plain with a maximum mound crest height of 3500 ms TWT at 65°S (e.g., CDP 3000 in Fig. 3).

Along the continental slope, a series of shelf-parallel, seaward-convex mounded high-relief sediment bodies (Fig. 1b, Fig. 6, Fig. 7g), separated by channels, is visible west of Darnley Drift along MacRobertson Land above reflector CS6. These mounds (Fig. 6) vary in appearance from east to west, showing geometries that are fairly symmetric (CDP 2500), asymmetric with a larger levee and steeper eastern flanks (CDP 4500), and flat topped (CDP 5200). Their surfaces are heavily scoured with a variety of moats that cut deeper in the eastern flanks.

6. Discussion

6.1. Seismic stratigraphic model

Horizon CS6 can be explained by the transition of the Mid-Miocene-Climatic-Optimum (MMCO) to the onset of renewed cooling (Shipboard Scientific Party, 2001a) transforming Antarctica's climate state from a coolhouse into an icehouse (Westerhold et al., 2020). The reflector is caused by a change of sedimentation processes ~14.3 Ma (CS6) (Cooper et al., 2008; Cooper and O'Brien, 2004; Hannah, 2006) from laminated contourites to hemipelagic and pelagic facies, accompanied by a large decrease in mass accumulation rate from 70 m/My in Unit III to 37 m/My Unit II (Handwerger and Jarrard, 2003).

Based on the occurrence of ice rafted debris in subunit IIC at ODP Site 1165 (seismic unit CS6-CS7) and an absence in subunit IIB, horizon CS7

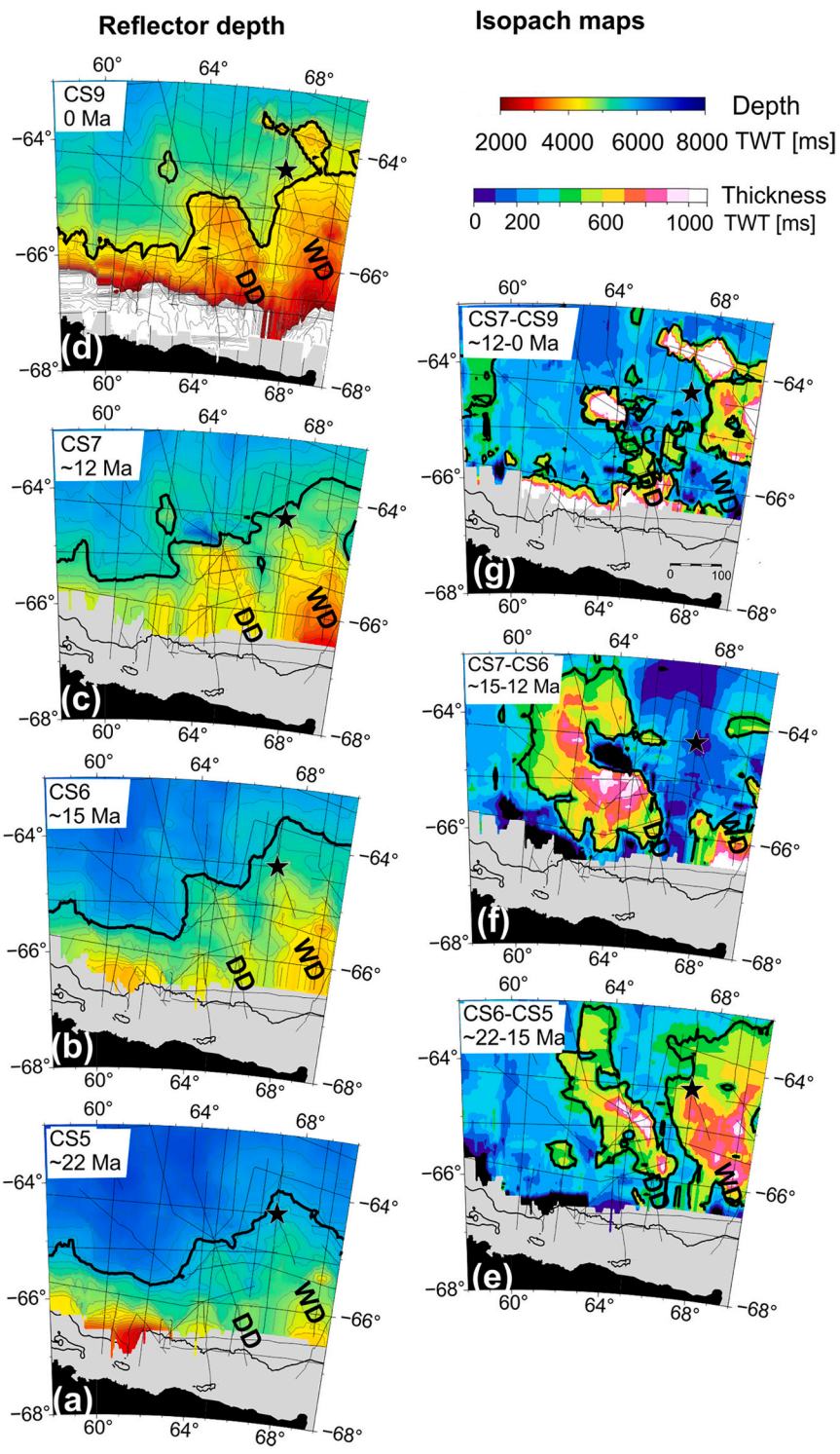

Fig. 7. Growth stages of Darnley Drift. Measured depths of reflectors CS5-CS9 (panels, a-d) and calculated isopach maps of seismic sequences CS5-CS6 to CS7-CS9 (panels, e-g) are given in TWT [ms] across the Darnley Drift and surrounding area off the MacRobertson Land (black area). Black thick line represents the root-mean-square (rms) values calculated for each depth and thickness slice, respectively. See text for further explanation. Areas with no data coverage are grey. ODP Site 1165 is marked with a black star. Straight, thin blue lines are the MCS profiles used to calculate the grids. Abbreviations: DD – Darnley Drift, WD – Wilkins/Wild Drift. (For interpretation of the references to colour in this figure legend, the reader is referred to the web version of this article.)

has been interpreted as the transition between a glacial and interglacial period (Shipboard Scientific Party, 2001b). An age estimation of this reflector is not straight forward, as it lies within a magnetic dissolution zone (Cooper et al., 2008). We assigned an age of 11.7 Ma to reflector CS7 (Table 2) based on a thickness of 138.4 m between reflectors CS7b and CS7 and a constant sedimentation rate of 37 m/My within lithological unit II (Cooper et al., 2008; Shipboard Scientific Party, 2001b). The prominent reflector CS7b at 114 mbsf/4917 ms TWT lies within Subunit IIA and has an age of ~8 Ma (Hannah, 2006). It is interpreted to be caused by a change in sedimentation rate to 20 m/My (Cooper et al., 2008) or 15 m/My (Shipboard Scientific Party, 2001b).

6.2. *Wild Canyon – a channel-levee complex*

In the early Miocene (initiated with reflector CS4a in Fig. 4) Wild Canyon formed as a channel-levee system (bottom panel in Fig. 9) with an asymmetric larger western levee characteristic for a an aggregational levee in a polar region, formed by overbank deposition during turbiditic events (Deptuck and Sylvester, 2018; Stow and Smillie, 2020). Similar examples have been reported around the continental margin of

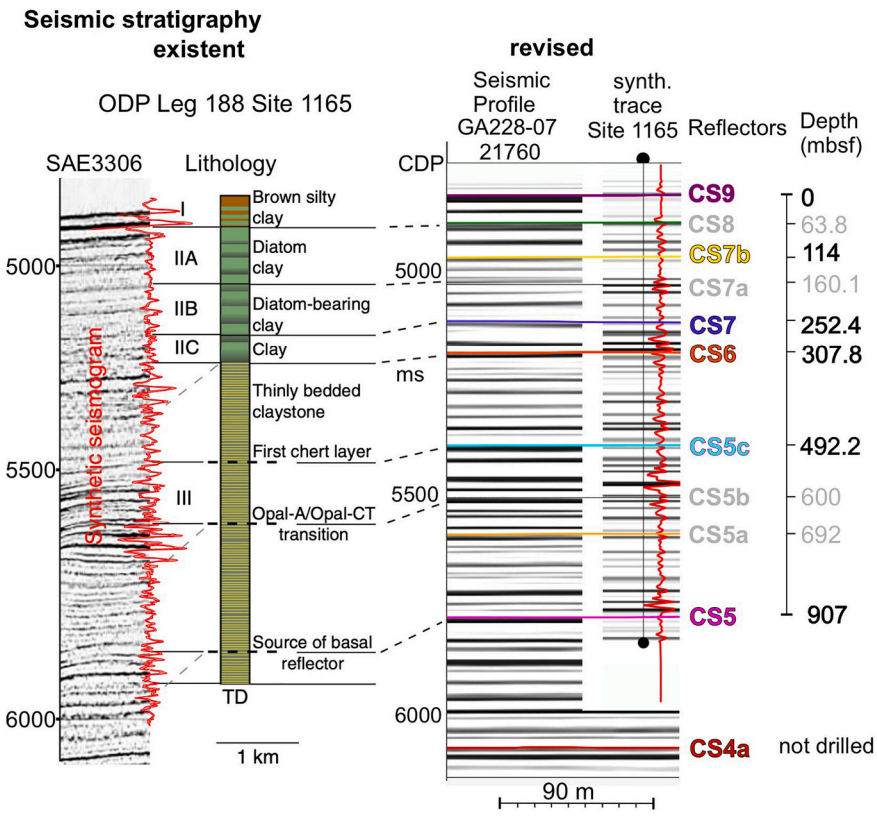

Fig. 8. Published lithostratigraphy of ODP Site 1165 (Shipboard Scientific Party, 2001b), seismic section SAE3306 and synthetic trace published by Handwerger et al. (2004) (left panel) compared to revised seismic stratigraphy in this study (right panel). Right panel: Calculated synthetic trace (red) incorporated into multi-channel seismic (MCS) reflection data of profile GA228–07. Naming of reflectors CS4-CS9 using extended version of nomenclature of (Leitchenkov et al., 2007), further explanation see text and Table 2. Colored reflectors are discussed in this study, grey reflectors are not. (For interpretation of the references to colour in this figure legend, the reader is referred to the web version of this article.)

Antarctica, for example in the adjacent Cosmonaut Sea (Kuvaas et al., 2004; Kuvaas and Leitchenkov, 1992). We thus interpret that the channel-levee system was formed by turbiditic activity.

An intensification of turbidity currents is imaged by growth and transformation of Wild Canyon from a channel-levee system into a submarine canyon at the continental slope-rise transition (seismic units CS5-CS6 and CS6-CS7) (Fig. 9). The transformation of Wild Canyon is recognized by large erosional features such as steep erosional flanks towards the western levee (Fig. 2-6) and slump deposits (Huang et al., 2020), causing Wild Canyon to at least double its size (Fig. 2-6, Fig. 7).

6.3. *Growth history of Darnley Drift as mixed-drift*

6.3.1. *CS5-CS6: early Miocene bottom current interaction with the channel-levee complex*

The isopach map of seismic sequences CS5-CS6 (Fig. 7e) and CS6-CS7 (Fig. 7f) shows a deflection of the western levee to the west. In addition to Coriolis force enhancing the deposition on the western levee (Deptuck and Sylvester, 2018), the deflection could be related to the basement topography and/or an interaction with bottom currents, most likely a combination of the three. Our dataset (Fig. 2-4) suggests that the location of the levee correlates with the orientation of the basement ridge (Supplementary material), which arcuate to the west at ~64.5°S and continues to strike northward at ~63°E. Sediments of seismic unit CS5-CS6 were preferentially deposited on top of the basement ridge and to its lee-side, as imaged on the isopach map (Fig. 7e). Basement topography marks a common morphological boundary condition for sedimentation and many examples around Antarctica have shown that sediment ridges as well as drift formation occur preferentially on the lee side of basement ridges (e.g., Huang and Jokat, 2016; Uenzelmann-Neben, 2006).

At the channel mouth (~64.5°S) where widening (Fig. 7e) occurs, we identify channel-lobes within seismic unit CS5-CS6 (Fig. 2-3, Fig. 7e) forming a sediment fan (Fig. 9). Sedimentary fan-lobes are caused by hemiturbiditic sediments settling from the suspension cloud, which can travel hundreds of kilometers (e.g., Stow and Smillie, 2020). Detailed seismic investigations of the Cosmonaut Sea Wedge further west between 35°-55° E have revealed analogue seismic characteristics, showing wedge-shaped, prograding sequences in the proximal part of the Cosmonaut Sea Wedge and a more sheeted deposition in the distal areas (Kuvaas et al., 2004; Kuvaas and Leitchenkov, 1992; Solli et al., 2008). The Cosmonaut Sea Wedge was interpreted as a marginal bottom-current reworked sediment fan-lobe with multiple depocenters.

The observed major shift of the sedimentary depocenter towards the western flank of the fan-lobe is a regional change that is contradictory to a sediment thickness distribution expected from hemiturbiditic deposition. Instead it is consistent with flow experiments by Miramontes et al. (2020) and studies of mixed turbiditic-contouritic drifts (Faugères et al., 1999, and references therein), showing changes of the turbidity deposits caused by a perpendicular bottom current. Depending on the strength of the bottom current, they can induce a shift of the channel fan deposits, interfinger with the turbiditic current or even cause areas of erosion (Faugères et al., 1999). We therefore conclude a current-reworked setting of the marginal sediment fan, similar to the Cosmonaut Sea Wedge (Kuvaas et al., 2004; Kuvaas and Leitchenkov, 1992; Solli et al., 2008). Based on the sediment thickness distribution in the isopach maps we further conclude that the interfingering of a westward flowing bottom current and the turbiditic current occurred at the channel mouth, where it contributed to the deflection of the channel-levee to the west (Fig. 9). This interpretation is supported by the occurrence of an elongated mounded drift (Fig. 3), which points towards a bottom current reworked sedimentation (Faugères et al., 1999; Faugères and Stow, 2008). Following the reflector depth and thickness contour lines of the sediment fan-lobe (Fig. 3, Fig. 7b and e), the bottom current continues northward at the mouth of Wild Canyon and to the west around the contours of the sediment fan, thus traveling south-west along its western margin. This caused a transformation of the sediment fan-lobes into a mixed fan-drift (Fig. 9).

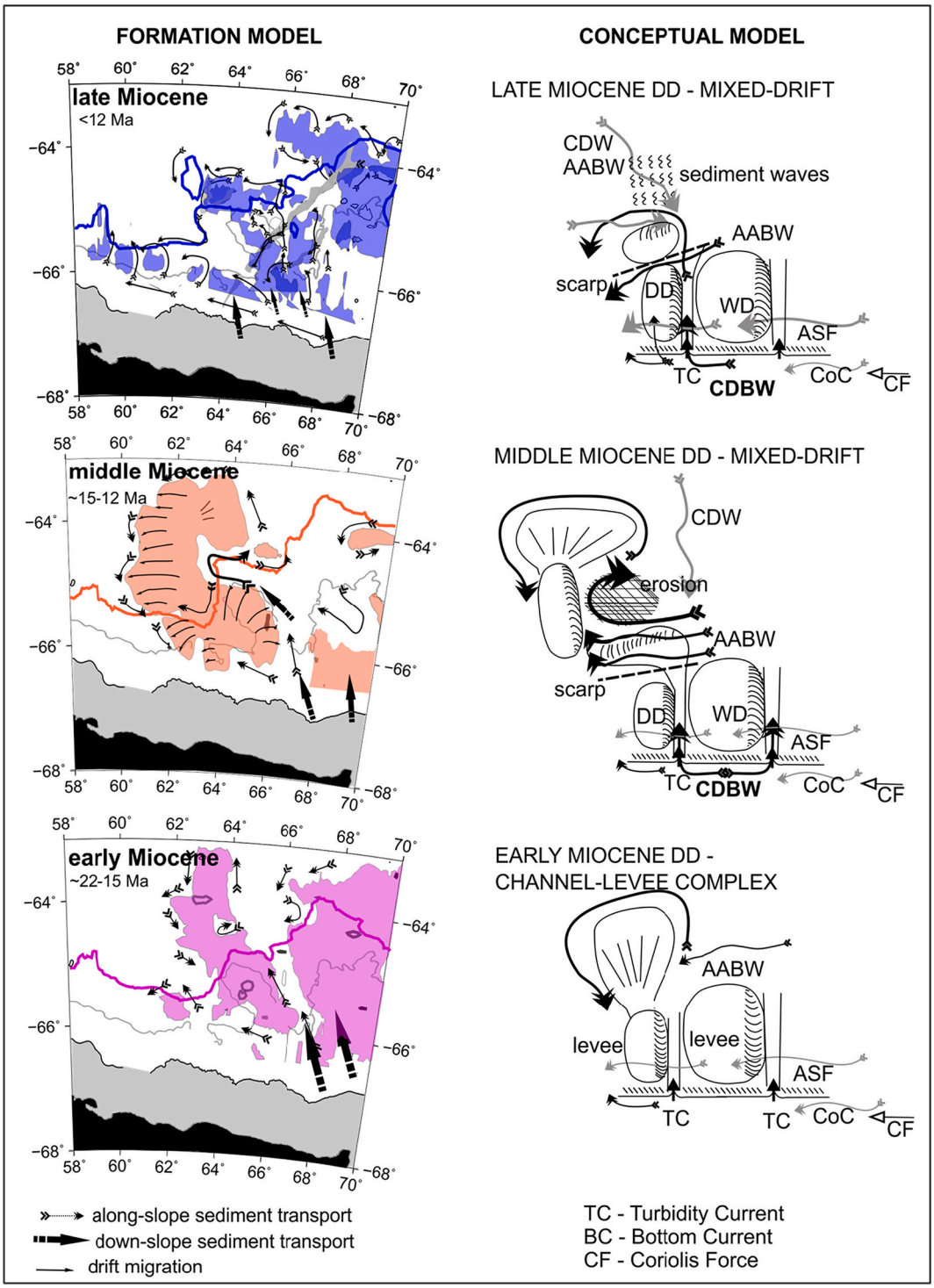

Fig. 9. Formation model (left side) and conceptual model (right side) of Darnley drift sediment sequences and bottom currents (black arrows), in particular Cape Darnley Bottom Water (CDBW) and CDW (grey arrows). Thick pink line marks the isoline of 5900 ms TWT for horizon CS5, the thick red line marks the isoline of 5560 ms TWT for horizon CS6 and the thick blue line marks the isoline of 5254 ms TWT for horizon CS7. Dark grey area shows bathymetric lows. Black area marks Antarctic continent, grey areas the shelf off the MacRobertson Land. Abbreviations: DD – Darnley Drift, WD – Wild Drift, CDW – Circumpolar Deep Water, AABW – Antarctic Bottom Water, ASF – Antarctic Slope Front, CoC – Antarctic Coastal Current. (For interpretation of the references to colour in this figure legend, the reader is referred to the web version of this article.)

6.3.2. CS6-CS7: middle Miocene mixed-drift formation

Levee deposits as well as drift deposits are recognized by characteristic internal seismic reflection pattern (Fig. 2-6) such as laterally continuous reflections and convex geometry, (e.g., Brackenridge et al., 2013; Faugères and Stow, 2008; Stow et al., 2002), which we observed for Darnley Drift above unconformity CS6. However, the observed mounded geometry, which shows a migration of the crest towards the abyssal plain and a gentle flank facing the continental shelf contradict a turbiditic deposition geometry that in general fades out towards the abyssal plain (Deptuck and Sylvester, 2018) but is instead a geometry characteristic for an elongated mounded drift body formed by bottom currents (Faugères et al., 1999; Faugères and Stow, 2008; Rebesco et al.,

1996). The shift of the sedimentary depocenter is comparable to the redeposition of another drift, Drift 7, located in the Antarctic Peninsula margin, where bottom currents have shifted the turbidity deposits to generate a gentle stoss side flank (Rebesco et al., 1996). In analogy, we interpret the gentle flank of Darnley Drift facing the stoss side of the bottom current, which is accordingly downslope along Wild Canyon (Fig. 9).

The observed initiation and growth of Darnley Drift body is supported by the sediment distribution observed in the isopach maps (Fig. 7f). At the channel mouth, the drift body correlates to an up to 1000 ms TWT thick, slope-parallel sediment accumulation. Seismic examples of drift body formation have shown that the direction of sediment aggradation image the predominant deposition regime (Faugères et al., 1999; Faugères and Stow, 2008; Stow et al., 2002), and is considered bottom current derived if the sediment body is elongated parallel to the slope along the depth contours (Uenzelmann-Neben, 2006). This leads to the interpretation that the growth of Darnley Drift is caused by a westward bottom current component at Wild Canyons channel mouth during the middle Miocene (Fig. 9).

The observed meander at the channel mouth is a common feature for deep-sea channel-canyon complexes and caused by irregularities, such as basement morphology (Amblas et al., 2018). In the meander, a current loses velocity and momentum to carry the sediment load in the inside bank. Thus, the deflection to the west allows sediment accumulate on Darnley Drift (Fig. 2-3), as seen by a change of the depocenter from a distribution parallel to Wild Canyon to a perpendicular one, parallel to the shelf (Fig. 2-3, Fig. 7f, Fig. 9). In this setup, the momentum is increased on the right-hand side in flow direction, which lead to non-deposition and erosion and suggests an intensification of the bottom current during the middle Miocene.

An additional current component is provided by a bottom current associated to AABW generated further east off Adélie and George V Land coast (Williams et al., 2010; Williams et al., 2008), interfingering at 63°E-65°E/64.5°S with the northward outflow of the bottom current along Wild Canyon. The jet of westward flowing AABW (Aoki et al., 2020; Heywood et al., 1999; Orsi et al., 1999) corresponds to an area of low- to non-deposition observed on Wild Drift and along Wild Canyon between 66°E-70°E/63°S-65.5°S (Fig. 7f) and seen as an angular unconformity in the seismic data (CDP 8600 in Fig. 4). It is consistent with literature examples of mixed-drift studies (e.g., Faugères et al., 1999; Faugères and Stow, 2008), where lateral shifts or interfingering of the turbiditic channel fan deposits were induced by bottom currents or areas of erosion or non-deposition were caused. The resulting intense bottom current followes the thickness contours at the mouth of Wild Canyon before it continues northwestward around the fan-drift of Darnley Drift (Fig. 7f and Fig. 9). It caused fan-drift deposits, that extended to about ~300 km in northwest-southeast direction and ~ 300 km to the west as derived from the seismic profiles and isopach maps in the lower continental rise between 64°S-63.5°S/62°E-65°E (Fig. 2 and Fig. 3, Fig. 7f). The same identification criteria as stated above have been applied, in particular geometry and seismic reflection characteristics such as an alternation of seismic transparent pattern topped by well-layered, mounded reflection patterns. Using our above interpretations, we conclude a major change in the predominant deposition regime from a turbidity one to a bottom current one. This caused a redeposition of the levee and fan sediments to form Darnley Drift as a mixed levee- elongated mounded drift at the continental slope-rise transition and mixed fan-drift in the lower continental rise (Fig. 9). Our findings are coherent with mixed turbiditic-contouritic systems indicating a higher energy depositional environment during aggrading periods (Cooper et al., 2008).

6.3.3. CS7-CS9 late predominant current controlled deposition

Shaped by bottom current controlled non-deposition and deposition, the ancient meander loop transformed into a channel, which caused a split-up of the paleo CDBW following the seafloor morphology with a major throughflow occurring to the west at ~64.5°S and a minor further north around the drift (Fig. 6). This caused a transformation of the sediment fan-drift into a separated drift (Fig. 7, Fig. 9). The paleo CDBW distribution is similar to recent CDBW distribution that reaches depth up to 4900 m (Aoki et al., 2020) and shows another ~2 km wide eastern channel-levee system (CDP 9300 in Fig. 5, Fig. 9).

Similar high-relief asymmetric mounded sedimentary bodies identified in the Cosmonaut Sea above a regional sediment lens have been interpreted as coalescing levee remnants and drift redeposition, with a larger component of down-slope turbidity current (Kuvaas et al., 2004; Kuvaas et al., 2005; Solli et al., 2008). Based on the mounded geometry and erosional features, we adopt this interpretation and suggest a mixed levee-drift formed by a slope parallel bottom current and downslope outflow of paleo-CDBW. At the slope rise transition, the observed slope-parallel channel of ~4 km width in a depth of 4500 ms TWT at the southern flank of Darnley Drift (Fig. 2 and Fig. 3) agrees well to AABW throughflow observed in moorings and CTD data (Mizuta et al., 2021; Nakayama et al., 2014). The outflow path along Wild Canyon, Daly canyon and the unnamed through in between agrees well to recent outflow of CDBW inferred from a bathymetry compilation (Smith et al., 2021). Recent CDBW is formed by mixing of DSW and CoC in the Burton and Nielsen basins (Fig. 1), and outflow occurs in the deep channels (Borchers et al., 2016). At the shelf break, paleo-CDBW is shifted to the west by the ASF (Jacobs, 1991; Middleton and Humphries, 1989).

6.4. Climatic context

We use the growth history of the Darnley Drift to mirror and discuss the evolution of the CDBW, its onset and changes in strength as well as pathways during warm and cold periods since the Oligocene-Miocene transition.

6.4.1. Oligocene/Miocene – mid Miocene (seismic sequence CS5 – CS6)

We calculated a mean thickness of 432 ms TWT for seismic unit CS5-CS6 (Fig. 7e), corresponding to a mean sedimentation rate of 86 m/My. This value lies within the published sedimentation rates on Wild Drift of 70 m/My to 120 m/My for this interval at ODP Site 1165 (Shipboard Scientific Party, 2001b). The large sediment supply has been related to multiple ice-advances of the EAIS onto the outer continental shelf (Cooper et al., 2008; Hannah, 2006; Shipboard Scientific Party, 2001b), providing a large supply of detritus and alternating facies of sand grains and granule to pebble sized dropstones. It reflects the establishment of a temperate to polythermal permanent ice sheet with a mass as great as 50% of Antarctica's present-day ice sheet, during the early Miocene, inferred from low $\delta^{18}O$ concentration (Zachos et al., 2001). The growth of the EAIS in the early Miocene caused incision of deep troughs transverse to the continental margin in East Antarctica, and massive erosion during this interval (Paxman et al., 2019). The channel-levee formation off MacRobertson Land continental shelf image the erosive character of the EAIS during the early Miocene that caused the transport of large amounts of sediment of continental origin onto the abyssal plain by turbidity currents. Post-18 Ma multiple ice sheet retreats occurred towards the Mid Miocene Climatic Optimum. Although, we were able to trace horizon CS5c on some profiles, which has an age of 17 Ma, in general we cannot distinguish this warming period due to the resolution limits.

The source of a bottom current remains hypothetic, but based on the paleo seafloor-depths during the early Miocene (Hochmuth et al., 2020), it is likely that the corresponding bottom water consisted of a northward directed turbiditic current that was mixed with circulated modified paleo-AABW entering Wild Canyon from the northern-eastern margin along Wild Drift. It is consistent to observed drift sediments at ODP Site 1165 (Handwerger et al., 2004). As any potential bottom current signature of CDBW descending Wild Canyon is small compared to the turbiditic outflow (Stow and Smillie, 2020), we cannot distinguish and identify any outflow of CDBW during the early Miocene.

6.4.2. Mid to late Miocene (Seismic unit CS6 – CS7)

Wild Canyons transformation of a channel into a canyon is consistent with a downslope model of canyon development. This model correlates erosion, enlarging and lengthening of the channels by turbidity currents to a shift of the source area to near the shelf edge due to a reduction in sea-level height (Amblas et al., 2018). This agrees well with climate models, which reveal an increase of $\delta^{18}O$ that was correlated to a sea-level drop caused by continent wide glaciation of Antarctica (Zachos et al., 2001; Zachos et al., 1992). It mirrors Antarctica's climatic transition from a coolhouse to icehouse around 13.9 Ma (Westerhold et al., 2020). During this dynamic cooling trend significant erosive ice-sheet expansion occurred on Antarctica (Haywood et al., 2009, and references therein), forming a quasi-permanent EAIS (Paxman et al., 2019; Siegert and Florindo, 2008) that was thicker and colder as during the early Miocene (Cooper et al., 2008; Paxman et al., 2019). During this transitional period, advancing of grounded ice caused bulldozing effects of the shelf sediments (Hannah, 2006) and prograding sediments (O'Brien et al., 2014) were deposited in sediment wedges at the continental shelf slope in Prydz Bay, MacRobertson Land (O'Brien et al., 2014) and Cosmonaut Sediment Wedge (Kuvaas et al., 2004; Solli et al., 2008). The erosive ice sheet launched dispersing icebergs with entrained sediments transporting recycled shelf deposits to ODP Site 1165 (Cooper et al., 2008; Hannah, 2006; Shipboard Scientific Party, 2001b). We have calculated an overall sedimentation rate off MacRobertson Shelf of ~150 m./My based on the mean thickness of 432 ms TWT of seismic sequence CS6-CS7 and velocities and age values provided in Table 2. This high value point to erosive glaciation that fit into this dynamic climatic scenario of Antarctica's rapid cooling and transition from a wet-based, polythermal, dynamic glaciation regime to a cold based and stable glaciation (Flower and Kennett, 1994).

6.4.2.1. Initiation of CDBW. The mid- to late Miocene seismic sequence CS6-CS7 represents a period of transitional deposition regime (Fig. 7f and Fig. 9) where we identify the development of Wild Canyon and simultaneous levee and drift formation of Darnley Drift as a mixed-drift. Based on Darnley Drift's growth history (seismic sequence CS6-CS7) as a levee-drift at the upper continental rise and a fan-drift in the lower continental rise, in the previous sections we have argued for a coexistence of turbidity and bottom currents descending Wild Canyon during the middle Miocene (14.9–11.7 Ma). We further inferred a shift of the dominant current regime from a turbiditic one at ~14.3 Ma to a bottom current one until ~11.7 Ma, which possible reflects Antarctica's transition into an icehouse world with a cold-based EAIS (Paxman et al., 2019; Westerhold et al., 2020). The bottom current signature increased around 12.7 Ma, observed by drift formation in the abyssal plain (Fig. 7g)Fig. 9, which coincidence with this transition around ~13.9 Ma, (Westerhold et al., 2020). Erosion rates of East Antarctica dropped to ~10 m/My (Paxman et al., 2019), which was also reported via detrital thermochronology data from Prydz Bay (Tochilin et al., 2012) and by a large drop of sedimentation rate to 37 m/My as well as a hiatus observed at ODP Site 1165 (star in Fig. 7f) during the middle Miocene (Florindo et al., 2003; Shipboard Scientific Party, 2001b). The growth of the Darnley Drift levee-drift between 14.9 and 11.7 Ma coincides with Antarctica's climatic transition and archives palaeo- CDBW outflow along Wild Canyon. As sea ice formation and the formation of DSW are preconditions for CDBW formation (Hirano et al., 2015; Mizuta et al., 2021; Nakayama et al., 2014), we can hence conclude that sea ice formation in the Cape Darnley Polynya region occurred and DSW was formed in the middle Miocene, prior to 11.7 Ma.

6.4.3. Late Miocene to recent (Seismic unit CS7 – CS9)

Our findings suggest similar production conditions of paleo-CDBW to today, which implies equivalent paleo climate conditions on the continental shelf off MacRobertson Land. Global changes in temperature, climate and ecosystems occurred in the late Miocene/Pliocene (e.g., Herbert et al., 2016; Ohneiser et al., 2015). Both North and South hemispheres cooled synchronously and ocean temperatures reached near-modern values between 7 and 5.4 Ma (Herbert et al., 2016), probably caused by a decline in atmospheric CO_2 level between 8 and 6 Ma. An increase of deep-current velocities is inferred from deep-ocean succession at Site 1165, which indicates a growth of Antarctic Ice volume after 6 Ma (Ohneiser et al., 2015). Ice rafting debris seen in sediments retrieved at Sites 745 and 746 at the Kerguelen Plateau reveal repeated ice advances with maxima between 8.8 Ma and 4.4 Ma and a reduction of ice rafts during late Pliocene/Quaternary (Ehrmann et al., 1991). Nielsen and Burton basins have been glacially eroded and overdeepened since the late Miocene, forming submarine glacial troughs (Cooper and O'Brien, 2004; O'Brien et al., 2014). This described icehouse world scenario of East Antarctica supports our findings of paleo-CDBW outflow along Wild Canyon, Daly Canyon and smaller unnamed canyons.

We interpret the sediment mound with the circle shaped center and elongated side lobes to be sediment drifts based on seismic reflection characteristics, described in previous studies (Kuvaas et al., 2004; Kuvaas and Leitchenkov, 1992; Leitchenkov et al., 2007). They concluded that the 1500 m thick sediment mound has been deposited current-controlled, which has been supported by ODP Site 1165 sediments (Hannah, 2006). Sediments with a sedimentation rate of 15–37 m/My have been reported at Site 1165 for lithologic Units I and II (Hannah, 2006; Shipboard Scientific Party, 2001b), which showed occurrences of dropstones and dispersed sand grains, indicating ice rafting and a growth of Antarctic Ice volume after 6 Ma (Cooper and O'Brien, 2004). Based on the calculated age of ~11.7 Ma for reflector CS7, and an overall rms-thickness of 409 ms TWT (Fig. 7g), we calculated sedimentation rates of ~27 m/My for seismic sequence CS7-CS9, under the assumption of a constant sedimentation. This suggests a reduction of the turbiditic contribution and an intensification of bottom current controlled deposition. It agrees well to an intensification of the ACC, the ASC and AABW since the late Miocene to early Pliocene observed in the sediment succession at ODP Site 1165 (Hannah, 2006).

We suggest the drift body is formed by a complex throughflow of paleo CDBW and AABW from Prydz Bay (Handwerger et al., 2004), which occurred through a buried canyon (~6 Ma) in the abyss of Prydz Bay (Kuvaas and Leitchenkov, 1992; Mizukoshi et al., 1986). This scenario (Fig. 6) is consistent with CTD measurements of recent CDBW and AABW at the northern margin of Wild Drift, which have revealed the existence of either a smaller amount of CDBW and/or newly formed AABW from Prydz Bay (Mizuta et al., 2021; Williams et al., 2016).

7. Conclusion

To reconstruction the development (initiation and modification in pathway and intensity) of CDBW during the Miocene transition from cool- to icehouse, we studied the spatial and chronological formation of a mixed-drift body, called Darnley Drift, off the MacRobertson Land Shelf. We utilized a combination of 13.350 km of multichannel-seismic reflection data, lithostratigraphic, and geological information of ODP Site 1165.

During the early Miocene (seismic unit CS5-CS6), the formation of Wild Canyon as channel-levee complex off MacRobertson Land shelf (Fig. 9) reflects Antarctica's cooling and establishment of a permanent polythermal ice-sheet (e.g., Zachos et al., 2001) that involved a large sediment transport (sedimentation rate of 86 m/My) through Wild Canyon as turbiditic currents and overbank deposition below Darnley Drift and Wild Drift. However, we could not identify any signs of paleo-CDBW outflow along Wild Canyon along the upper continental rise, specifically no drift formation in the area of today's Darnley Drift. This suggests, that no or less DSW was produces and consequently no intense sea-ice formation occurred in the Cape Darnley Polynya.

A mixed-fan drift established on the lower continental rise (north of the pink thick line in Fig. 9), that could be attributed to an interfingering

of the turbiditic current descending down Wild Canyon and a paleo-AABW towards the west along the contours of Darnley Drift.

During the mid-Miocene (seismic unit CS6-CS7), we observed a transitional period of mixed-drift formation with turbiditic currents and bottom currents coexisting along Wild Canyon. An unconformity can be observed within seismic sequence CS6-CS7 (Fig. 2-6), above which bottom currents became the dominant current regime. Timing suggests a linkage to Antarctica's climatic transition from coolhouse to icehouse at ~13.9 Ma (Westerhold et al., 2020) that involved a transition from a wet-based, polythermal, dynamic glaciation regime to a cold based and stable glaciation that included intense sea ice and DSW formation in the Cape Darnley Polynya. Paleo-CDBW outflow was either initiated and/or intensified during this period resulting in the formation of Darnley Drift as an elongated mounded drift body at the upper continental rise. Paleo-CDBW mixing with paleo-AABW continued north- and westward around Darnley Drift as a bottom current, thereby depositing a mixed fan-drift in the lower continental rise and causing a growth to a maximum extent of ~60,000 km^2 (Fig. 7f and Fig. 9).

The late Miocene and younger (11.7–0 Ma) sedimentary sequence (seismic unit CS7-CS9) shows a distinct depositional change characterized by a decrease in sedimentation rate to 27 m/My, and the development of distinct sediment drifts located at the northern termination of Darnley Drift at 65°S and at the northern part of Wild Drift. At the continental rise, a series of mixed-channel-levee-drifts can be inferred. We concluded an intensity increase of various bottom currents, including CDBW and AABW.

Data availability statement

The presented multichannel seismic reflection data can be downloaded from the Antarctic Seismic Data Library System (SDLS) https://sdls.ogs.trieste.it/cache/index.jsp (Wardell et al., 2007). Logging data of Leg 188 Site 1165, which were used for the calculation of the synthetic seismogram, were generated and published by Handwerger et al. (2004).

Author contribution

R. Nielsen interpreted the seismic reflection data and provided the conceptual design of this study. R. Nielsen wrote the draft of the manuscript, which was critically revised by G. Uenzelmann-Neben. All authors contributed to the article and approved the submitted version. The project was initiated by G. Uenzelmann-Neben.

Funding

The project is funded by the Alfred Wegener Institute, Helmholtz Center for Polar- and Marine Science.

Declaration of Competing Interest

The authors declare that they have no known competing financial interests or personal relationships that could have appeared to influence the work reported in this paper.

Acknowledgments

The authors would like to thank Emerson E&P Software, Emerson Automation Solutions, for providing licenses of the seismic software Paradigm in the scope of the Emerson Academic Program. This work used data provided by the Ocean Drilling Project (ODP).

Appendix A. Supplementary data

Supplementary data to this article can be found online at https://doi.org/10.1016/j.margeo.2022.106735.

References

Amblas, D., Ceramicola, S., Gerber, T.P., Canals, M., Chiocci, F.L., Dowdeswell, J.A., Harris, P.T., Huvenne, V.A.I., Lai, S.Y.J., Lastras, G., Iacono, C.L., Micallef, A., Mountjoy, J.J., Paull, C.K., Puig, P., Sanchez-Vidal, A., 2018. Submarine Canyons and Gullies. In: Micallef, A., Krastel, S., Savini, A. (Eds.), Submarine Geomorphology. Springer International Publishing, Cham, pp. 251–272.

Aoki, S., Katsumata, K., Hamaguchi, M., Noda, A., Kitade, Y., Shimada, K., Hirano, D., Simizu, D., Aoyama, Y., Doi, K., Nogi, Y., 2020. Freshening of Antarctic bottom water off Cape Darnley, East Antarctica. J. Geophys. Res. Oceans 125 e2020JC016374.

Bindoff, N.L., Rosenberg, M.A., Warner, M.J., 2000. On the circulation and water masses over the Antarctic continental slope and rise between 80 and 150°E. Deep-Sea Res. II Top. Stud. Oceanogr. 47, 2299–2326.

Borchers, A., Voigt, I., Kuhn, G., Diekmann, B., 2011. Mineralogy of glaciomarine sediments from the Prydz Bay-Kerguelen region: relation to modern depositional environments. Antarct. Sci. 23, 164–179.

Borchers, A., Dietze, E., Kuhn, G., Esper, O., Voigt, I., Hartmann, K., Diekmann, B., 2016. Holocene ice dynamics and bottom-water formation associated with Cape Darnley polynya activity recorded in Burton Basin, East Antarctica. Mar. Geophys. Res. 37, 49–70.

Brackenridge, R.E., Hernández-Molina, F.J., Stow, D.A.V., Llave, E., 2013. A Pliocene mixed contourite–turbidite system offshore the Algarve Margin, Gulf of Cadiz: Seismic response, margin evolution and reservoir implications. Mar. Pet. Geol. 46, 36–50.

Cooper, A.K., O'Brien, P., 2004. Leg 188 synthesis: transitions in the glacial history of the Prydz Bay Region, East Antarctica, from ODP Drilling. Proc. Ocean Drill. Program: Sci. Results 188, 1–42.

Cooper, A.K., Barrett, P.J., Hinz, K., Traube, V., Letichenkov, G., Stagg, H.M.J., 1991. Cenozoic prograding sequences of the Antarctic continental margin: a record of glacio-eustatic and tectonic events. Mar. Geol. 102, 175–213.

Cooper, A.K., Brancolini, G., Escutia, C., Kristoffersen, Y., Larter, R., Leitchenkov, G., O'Brien, P., Jokat, W., 2008. Chapter 5 Cenozoic climate history from seismic reflection and drilling studies on the antarctic continental margin. In: Florindo, F., Siegert, M. (Eds.), Developments in Earth and Environmental Sciences. Elsevier, pp. 115–234.

Covault, J., 2011. Submarine fans and canyon-channel systems: A review of processes, products, and models. Nat. Educ. Knowledge 3 (10), 4.

Deptuck, M.E., Sylvester, Z., 2018. Submarine Fans and their channels, levees, and lobes. In: Micallef, A., Krastel, S., Savini, A. (Eds.), Submarine Geomorphology. Springer International Publishing, Cham, pp. 273–299.

Ehrmann, W., Grobe, H., Fütterer, D., 1991. Late Miocene to Holocene glacial history of East Antarctica revealed by sediments from Sites 745 and 746. Proc., scientific results, ODP, Leg 119, Kerguelen Plateau-Prydz Bay.

Erohina, T., Cooper, A., Handwerger, D., Dunbar, R., 2004. Seismic stratigraphic correlations between ODP sites 742 and 1166: implications for depositional paleoenvironments in Prydz Bay, Antarctica. Proc. ODP Sci. Results 188, 1–21.

Esentia, I., Stow, D., Smillie, Z., 2018. Contourite drifts and associated bedforms. In: Micallef, A., Krastel, S., Savini, A. (Eds.), Submarine Geomorphology. Springer International Publishing, Cham, pp. 301–331.

Faugères, J.C., Stow, D.A.V., 2008. Chapter 14 Contourite drifts: nature, evolution and controls. In: Rebesco, M., Camerlenghi, A. (Eds.), Developments in Sedimentology. Elsevier, pp. 257–288.

Faugères, J.-C., Stow, D.A.V., Imbert, P., Viana, A., 1999. Seismic features diagnostic of contourite drifts. Mar. Geol. 162, 1–38.

Florindo, F., Bohaty, S.M., Erwin, P.S., Richter, C., Roberts, A.P., Whalen, P.A., Whitehead, J.M., 2003. Magnetobiostratigraphic chronology and palaeoenvironmental history of Cenozoic sequences from ODP sites 1165 and 1166, Prydz Bay, Antarctica. Palaeogeogr. Palaeoclimatol. Palaeoecol. 198, 69–100.

Flower, B.P., Kennett, J.P., 1994. The middle Miocene climatic transition: East Antarctic ice sheet development, deep ocean circulation and global carbon cycling. Palaeogeogr. Palaeoclimatol. Palaeoecol. 108, 537–555.

Gill, A.E., 1973. Circulation and bottom water production in the Weddell Sea. Deep-Sea Res. Oceanogr. Abstr. 20, 111–140.

Handwerger, D.A., Jarrard, R.D., 2003. Neogene changes in Southern Ocean sedimentation based on mass accumulation rates at four continental margins. Paleoceanography 18.

Handwerger, D., Cooper, A., O'Brien, P., Williams, T., Barr, S., Dunbar, R., Leventer, A., Jarrard, R., 2004. Synthetic seismograms linking ODP sites to seismic profiles, continental rise and shelf of Prydz Bay, 188. Antarctica. Proc. ODP, Scientific Results.

Hannah, M.J., 2006. The palynology of ODP site 1165, Prydz Bay, East Antarctica: a record of Miocene glacial advance and retreat. Palaeogeogr. Palaeoclimatol. Palaeoecol. 231, 120–133.

Harris, P.T., O'Brien, P.E., 1996. Geomorphology and sedimentology of the continental shelf adjacent to Mac. Robertson Land, East Antarctica: a scalped shelf. Geo-Mar. Lett. 16, 287–296.

Harris, P.T., O'Brien, P.E., 1998. Bottom currents, sedimentation and ice-sheet retreat facies successions on the Mac Robertson shelf, East Antarctica. Mar. Geol. 151, 47–72.

Haywood, A., Smellie, J., Ashworth, A., Cantrill, D., Fabio, F., Hambrey, M., Hill, D., Hillenbrand, C., Hunter, S., Larter, R., et al., 2009. Chapter 10 Middle Miocene to Pliocene History of Antarctica and the Southern Ocean. In: Florindo, F., Siegert, M. (Eds.), Developments in Earth and Environmental Sciences. Elsevier, pp. 401–463.

Herbert, T., Lawrence, K., Tzanova, A., Peterson, L., Caballero-Gill, R., Kelly, C., 2016. Late Miocene global cooling and the rise of modern ecosystems. Nat. Geosci. 9.

Heywood, K.J., Sparrow, M.D., Brown, J., Dickson, R.R., 1999. Frontal structure and Antarctic Bottom Water flow through the Princess Elizabeth Trough, Antarctica. Deep-Sea Res. I Oceanogr. Res. Pap. 46, 1181–1200.
Hirano, D., Kitade, Y., Ohshima, K.I., Fukamachi, Y., 2015. The role of turbulent mixing in the modified Shelf Water overflows that produce Cape Darnley Bottom Water. J. Geophys. Res. Oceans 120, 910–922.
Hochmuth, K., Gohl, K., Leitchenkov, G., Sauermilch, I., Whittaker, J., Uenzelmann-Neben, G., Davy, B., Santis, L., 2020. The Evolving paleobathymetry of the circum-Antarctic Southern Ocean Since 34 Ma: a key to understanding past cryosphere-ocean developments. Geochem. Geophys. Geosyst. 21.
Huang, X., Jokat, W., 2016. Middle Miocene to present sediment transport and deposits in the Southeastern Weddell Sea, Antarctica. Glob. Planet. Chang. 139, 211–225.
Huang, X., Bernhardt, A., Santis, L., Wu, S., Leitchenkov, G., Harris, P., O'Brien, P., 2020. Depositional and erosional signatures in sedimentary successions on the continental slospe and rise off Prydz Bay, East Antarctica– implications for Pliocene paleoclimate. Mar. Geol. 430.
Jacobs, S.S., 1991. On the nature and significance of the Antarctic Slope Front. Mar. Chem. 35, 9–24.
Jacobs, S.S., Amos, A.F., Bruchhausen, P.M., 1970. Ross sea oceanography and antarctic bottom water formation. Deep-Sea Res. Oceanogr. Abstr. 17, 935–962.
Joshima, M., Ishihara, T., Nakajima, T., Sugiyama, K., Tsuchida, K., Kato, A., Murakami, F., Brown, B., 2001. Preliminary results of the TH99 geological and geophysical survey in the Cooperation Sea and Prydz Bay area. Polar Geosci. 14, 244–262.
Kuvaas, B., Leitchenkov, G., 1992. Glaciomarine turbidite and current controlled deposits in Prydz Bay, Antarctica. Mar. Geol. 108, 365–381.
Kuvaas, B., Kristoffersen, Y., Guseva, J., Leitchenkov, G., Gandjukhin, V., Kudryavtsev, G., 2004. Input of glaciomarine sediments along the East Antarctic continental margin; depositional processes on the Cosmonaut Sea continental slope and rise and a regional acoustic stratigraphic correlation from 40° W to 80° E. Mar. Geophys. Res. 25, 247–263.
Kuvaas, B., Kristoffersen, Y., Guseva, J., Leitchenkov, G., Gandjukhin, V., Løvås, O., Sand, M., Brekke, H., 2005. Interplay of turbidite and contourite deposition along the Cosmonaut Sea/Enderby Land margin, East Antarctica. Mar. Geol. 217, 143–159.
Leitchenkov, G., Stagg, H., Gandjukhin, V., Cooper, A.K., Tanahashi, M., O'Brien, P., 1994. Cenozoic seismic stratigraphy of Prydz Bay (Antarctica). Terra Antarct. 1, 395–397.
Leitchenkov, G., Guseva, Y.B., Gandyukhin, V.V., 2007. Cenozoic environmental changes along the East Antarctic continental margin inferred from regional seismic stratigraphy, Short Research Paper U.S. Geological Survey and The National Academies. USGS, pp. 395–397.
Middleton, J.H., Humphries, S.E., 1989. Thermohaline structure and mixing in the region of Prydz Bay, Antarctica. Deep-Sea Res.A-Oceanographic Research Papers 36, 1255–1266.
Miramontes, E., Eggenhuisen, J.T., Jacinto, R.S., Poneti, G., Pohl, F., Normandeau, A., Campbell, D.C., Hernández-Molina, F.J., 2020. Channel-levee evolution in combined contour current–turbidity current flows from flume-tank experiments. Geology 48, 353–357.
Mizukoshi, I., Sunouchi, H., Saki, T., Sato, S., Tanahashi, M., 1986. Preliminary report of geological and geophysical surveys off Amery Ice Shelf, East Antarctica. Memoirs of National Institute of Polar Research. Special issue 43, 48–61.
Mizuta, G., Fukamachi, Y., Simizu, D., Matsumura, Y., Kitade, Y., Hirano, D., Fujii, M., Nogi, Y., Ohshima, K.I., 2021. Seasonal evolution of Cape Darnley bottom water revealed by mooring measurements. Front. Mar. Sci. 8.
Nakayama, Y., Ohshima, K.I., Matsumura, Y., Fukamachi, Y., Hasumi, H., 2014. A numerical investigation of formation and variability of Antarctic Bottom Water off Cape Darnley, East Antarctica. J. Phys. Oceanogr. 44, 2921–2937.
O'Brien, P.E., Cooper, A., Fabio, F., Handwerger, D.A., Lavelle, M., Passchier, S., Pospichal, J.J., Quilty, P., Richter, C., Theissen, K., others, 2004. Prydz Channel Fan and the History of Extreme Ice Advances in Prydz BayProc. ODP Sci. Results 188, 1–32.
O'Brien, P.E., Harris, P.T., Post, A.L., Young, N., 2014. Chapter 18 East Antarctic continental shelf: Prydz Bay and the Mac.Robertson Land Shelf. Geol. Soc. Lond. Mem. 41, 241–254.
Ohneiser, C., Florindo, F., Stocchi, P., Roberts, A.P., DeConto, R.M., Pollard, D., 2015. Antarctic glacio-eustatic contributions to late Miocene Mediterranean desiccation and reflooding. Nat. Commun. 6, 8765.
Ohshima, K.I., Fukamachi, Y., Williams, G.D., Nihashi, S., Roquet, F., Kitade, Y., Tamura, T., Hirano, D., Herraiz-Borreguero, L., Field, I., Hindell, M., Aoki, S., Wakatsuchi, M., 2013. Antarctic Bottom Water production by intense sea-ice formation in the Cape Darnley polynya. Nat. Geosci. 6, 235.
Orsi, A.H., Whitworth, T., Nowlin, W.D., 1995. On the meridional extent and fronts of the Antarctic Circumpolar Current. Deep-Sea Res. I Oceanogr. Res. Pap. 42, 641–673.
Orsi, A.H., Johnson, G.C., Bullister, J.L., 1999. Circulation, mixing, and production of Antarctic Bottom Water. Prog. Oceanogr. 43, 55–109.
Passchier, S., 2011. Linkages between East Antarctic Ice Sheet extent and Southern Ocean temperatures based on a Pliocene high-resolution record of ice-rafted debris off Prydz Bay, East Antarctica. Paleoceanography 26, 1–13.
Paxman, G.J.G., Jamieson, S.S.R., Hochmuth, K., Gohl, K., Bentley, M.J., Leitchenkov, G., Ferraccioli, F., 2019. Reconstructions of Antarctic topography since the Eocene–Oligocene boundary. Palaeogeogr. Palaeoclimatol. Palaeoecol. 535, 109346.
Rahmstorf, S., 2006. Thermohaline ocean circulation. Encyclopedia Quatern. Sci. 5.
Rebesco, M., Larter, R.D., Camerlenghi, A., Barker, P.F., 1996. Giant sediment drifts on the continental rise west of the Antarctic Peninsula. Geo-Mar. Lett. 16, 65–75.
Rintoul, S.R., 1998. On the Origin and Influence of Adélie Land Bottom Water, Ocean, Ice, and Atmosphere: Interactions at the Antarctic Continental Margin, pp. 151–171.
Shipboard Scientific Party, 2001a. Leg 188 Summary: Prydz Bay - Cooperation Sea, Antarctica. In: O'Brien, P., Cooper, A.K., Richter, C., et al. (Eds.), Proceedings of the Ocean Drilling Program, Initial Reports. College Station TX 77845–9547. Texas A&M University, USA, pp. 1–65.
Shipboard Scientific Party, 2001b. Site 1165. In: O'Brien, P., Cooper, A.K., Richter, C., et al. (Eds.), Proceedings of the Ocean Drilling Program, Initial Reports. College Station TX 77845–9547, USA. Texas A&M University, pp. 1–191.
Siegert, M.J., Florindo, F., 2008. Chapter 1 Antarctic climate evolution. In: Florindo, F., Siegert, M. (Eds.), Developments in Earth and Environmental Sciences. Elsevier, pp. 1–11.
Smith, N.R., Zhaoqian, D., Kerry, K.R., Wright, S., 1984. Water masses and circulation in the region of Prydz Bay, Antarctica. Deep Sea Res. A. Oceanogr. Res. Papers 31, 1121–1147.
Smith, J., Nogi, Y., Spinoccia, M., Dorschel, B., Leventer, A., 2021. A bathymetric compilation of the Cape Darnley region, East Antarctica. Antarct. Sci. 1–12.
Solli, K., Kuvaas, B., Kristoffersen, Y., Leitchenkov, G., Guseva, J., Gandjukhin, V., 2008. The Cosmonaut Sea Wedge. Mar. Geophys. Res. 29, 51–69.
Stagg, H.M.J., 1985. The structure and origin of Prydz Bay and MacRobertson Shelf, East Antarctica. Tectonophysics 114, 315–340.
Stow, D., Smillie, Z., 2020. Distinguishing between Deep-Water sediment facies: turbidites, contourites and hemipelagites. Geosciences 10, 68.
Stow, D.A.V., Faugeres, J.-C., Howe, J.A., Pudsey, C.J., Viana, A.R., 2002. Bottom currents, contourites and deep-sea sediment drifts: current state-of-the-art. In: Stow, D.A.V., Pudsey, C.J., Howe, J.A., Faugeres, J.C., Viana, A.R. (Eds.), Deep-Water Contourite Systems: Modern Drifts and Ancient Series, Seismic and Sedimentary Characteristics. Geological Society of London, pp. 7–20.
Tochilin, C.J., Reiners, P.W., Thomson, S.N., Gehrels, G.E., Hemming, S.R., Pierce, E.L., 2012. Erosional history of the Prydz Bay sector of East Antarctica from detrital apatite and zircon geo- and thermochronology multidating. Geochem. Geophys. Geosyst. 13.
Uenzelmann-Neben, G., 2006. Depositional patterns at Drift 7, Antarctic Peninsula: along-slope versus down-slope sediment transport as indicators for oceanic currents and climatic conditions. Mar. Geol. 233, 49–62.
Vaz, R.A.N., Lennon, G.W., 1996. Physical oceanography of the Prydz Bay region of Antarctic waters. Deep-Sea Research Part I-Oceanographic Research Papers 43, 603–641.
Wakatsuchi, M., Ohshima, K.I., Hishida, M., Naganobu, M., 1994. Observations of a street of cyclonic eddies in the Indian Ocean sector of the Antarctic Divergence. J. Geophys. Res. Oceans 99, 20417–20426.
Wardell, N., Childs, J.R., Cooper, A.K., 2007. Advances through collaboration: sharing seismic reflection data via the Antarctic Seismic Data Library System for Cooperative Research (SDLS). Open-File Report, Reston, VA.
Wessel, P., Luis, J.F., 2017. The GMT/MATLAB Toolbox. Geochem. Geophys. Geosyst. 18, 811–823.
Westerhold, T., Drury, A.J., Liebrand, D., Agnini, C., Anagnostou, E., Barnet, J., Bohaty, S., De Vleeschouwer, D., Fabio, F., Frederichs, T., Hodell, D., Holbourn, A., Kroon, D., Lauretano, V., Littler, K., Lourens, L., Lyle, M., Pälike, H., Zachos, J.C., 2020. An astronomically dated record of Earth's climate and its predictability over the last 66 million years. Science (New York, N.Y.) 369, 1383–1387.
Whitehead, J.M., Quilty, P.G., McKelvey, B.C., O'Brien, P.E., 2006. A review of the Cenozoic stratigraphy and glacial history of the Lambert Graben-Prydz Bay region, East Antarctica. Antarct. Sci. 18, 83–99.
Williams, G.D., Bindoff, N.L., Marsland, S.J., Rintoul, S.R., 2008. Formation and export of dense shelf water from the Adélie Depression, East Antarctica. J. Geophys. Res. Oceans 113.
Williams, G.D., Aoki, S., Jacobs, S.S., Rintoul, S.R., Tamura, T., Bindoff, N.L., 2010. Antarctic Bottom Water from the Adélie and George V Land coast, East Antarctica (140–149°E). J. Geophys. Res. Oceans 115.
Williams, G.D., Herraiz-Borreguero, L., Roquet, F., Tamura, T., Ohshima, K.I., Fukamachi, Y., Fraser, A.D., Gao, L., Chen, H., McMahon, C.R., Harcourt, R., Hindell, M., 2016. The suppression of Antarctic bottom water formation by melting ice shelves in Prydz Bay. Nat. Commun. 7.
Wong, A.P.S., Riser, S.C., 2013. Modified shelf water on the continental slope north of Mac Robertson Land, East Antarctica. Geophys. Res. Lett. 40, 6186–6190.
Zachos, J.C., Breza, J.R., Wise, S.W., 1992. Early Oligocene ice-sheet expansion on Antarctica: Stable isotope and sedimentological evidence from Kerguelen Plateau, southern Indian Ocean. Geology 20, 569–573.
Zachos, J., Pagani, M., Sloan, L., Thomas, E., Billups, K., 2001. Trends, rhythms, and aberrations in global climate 65 Ma to present. Science 292, 686–693.